



# Langmuir Solitons and their Role in Artificial Ionization in Ionospheric Heating Experiments

Dennis Papadopoulos  
University of Maryland

Symposium  
“The Power of Plasma Theory”  
Leonid Rudakov 80<sup>th</sup>  
May 4, 2013  
LaJolla, Ca

## Acknowledge:

B. Eliasson, C.L. Chang,  
G. Milikh, X. Shao, P. Bernhardt  
B. Watkins, T. Pedersen, E.Mishin



# LEONID RUDAKOV – ALWAYS AHEAD OF THE TIME

## WEAK TURBULENCE

### OSCILLATIONS AND INSTABILITY OF A WEAKLY TURBULENT PLASMA\*

A. A. VEDENOV, A. V. GORDEEV and L. I. RUDAKOV  
I. V. Kurchatov Institute of Atomic Energy, Moscow, U.S.S.R.

*(Received 19 November 1965)*

THE PURPOSE of this paper is to study the possibility of describing effects associated with the interaction of collective oscillations of a plasma by means of a self-consistent system of equations: a kinetic equation for the distribution function of high frequency waves (in six-dimensional co-ordinate and wave vector space) and equations describing the slow motion of a plasma under the action of a high frequency pressure. By means of such a system of equations it is possible to investigate processes in which the characteristic periods and wavelengths considerably exceed the period and wavelength of high frequency oscillations; only averaged characteristics of the high frequency waves enter into the equations, and under such conditions these may be considered as quasi-particles.

$$W / nT < (k\lambda_D)$$

## STRONG TURBULENCE

### Spectra of Strong Langmuir Turbulence\*

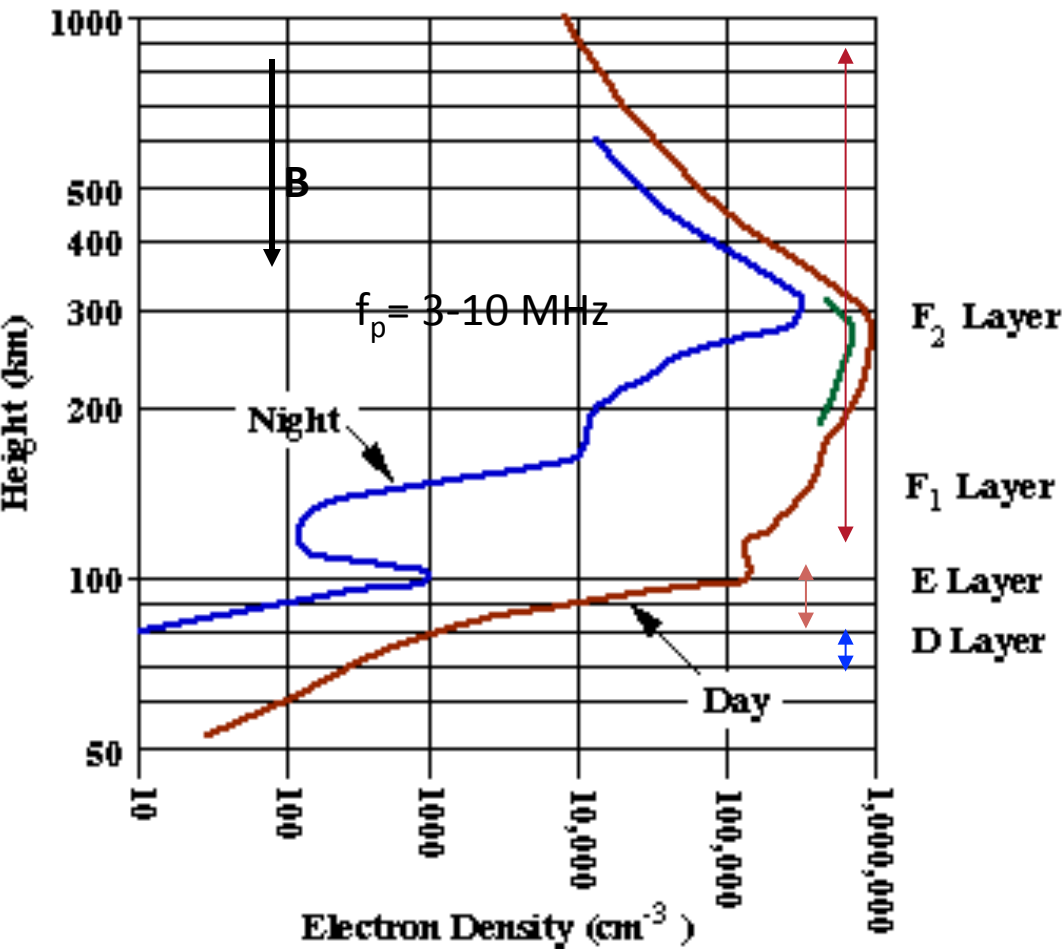
A. S. Kingsep,\* L. I. Rudakov,\* and R. N. Sudan†  
*International Centre for Theoretical Physics, Trieste, Italy*

*(Received 4 October 1973)*

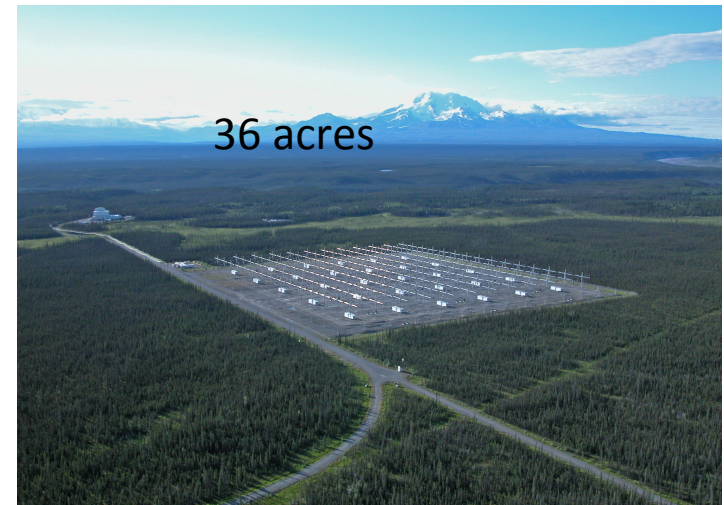
Strong Langmuir turbulence is described in terms of a random set of blobs of self-trapped plasma waves. The interaction of these blobs leads to the generation of power spectra  $\langle |E_k|^2 \rangle \propto k^{-2}$  that agree with the results of one-dimensional computer simulation.

$$W / nT > (k\lambda_D)$$

# IONOSPHERIC HEATING AND HEATERS



HAARP heater – Phase Array -360 el  
2.8-10 MHz, ERP .6-5 GW

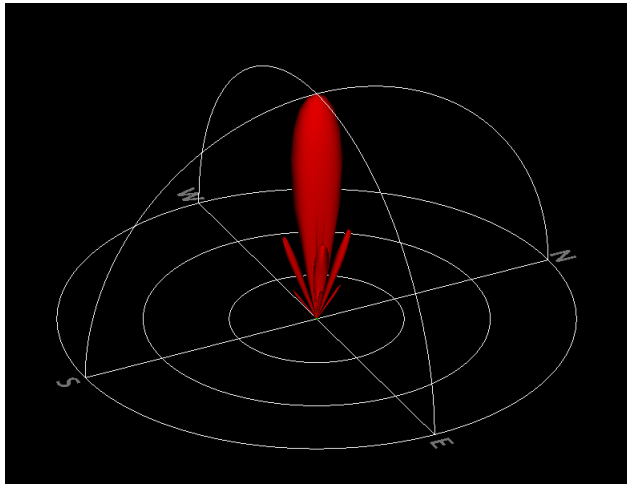


$E \approx 1-1.5 \text{ V/m}$  at 150 km, 5 MHz

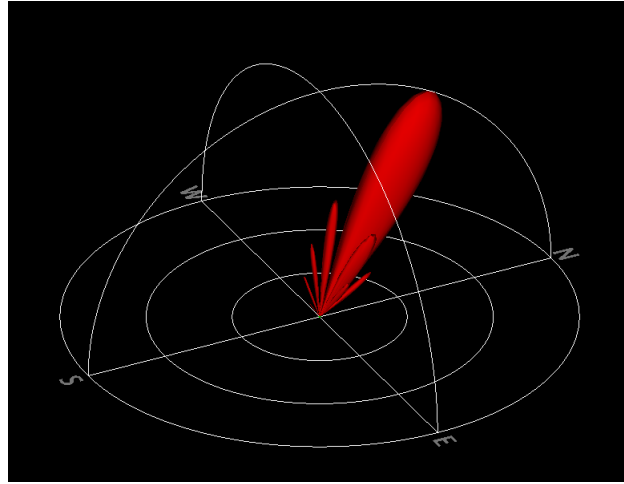
$$\tilde{V} / V_e \approx .1 \quad \text{at } 230 \text{ km}$$



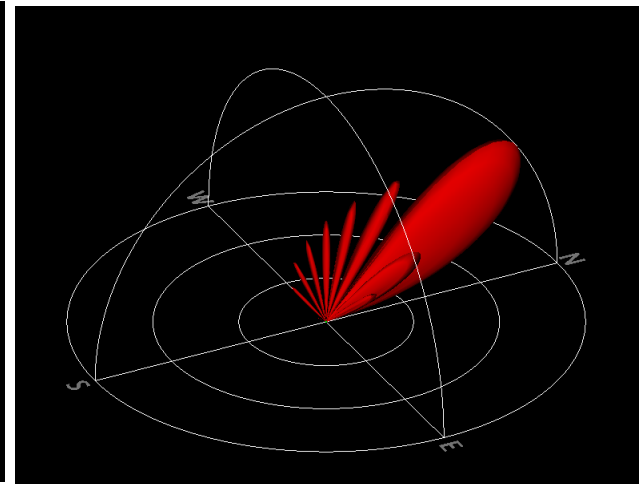
# 4.5 MHz, Azimuth=0



Zenith = 0

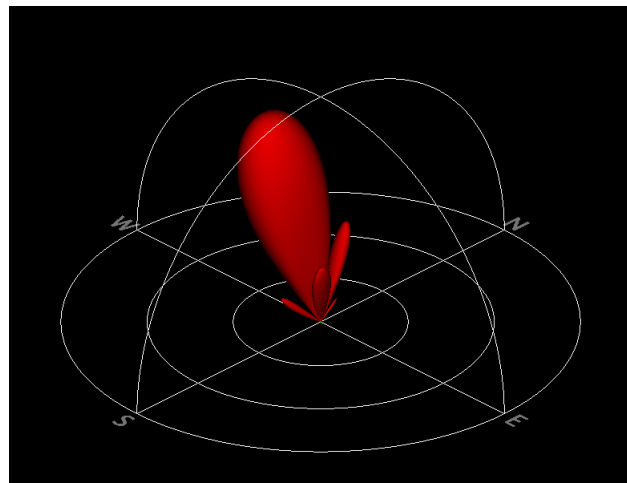


Zenith=45

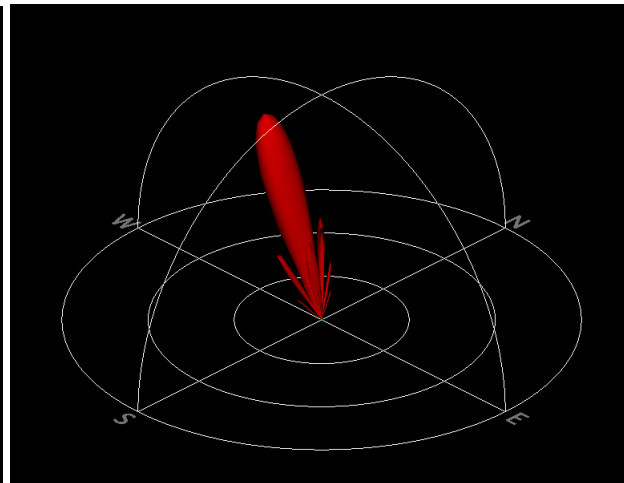


Zenith=60

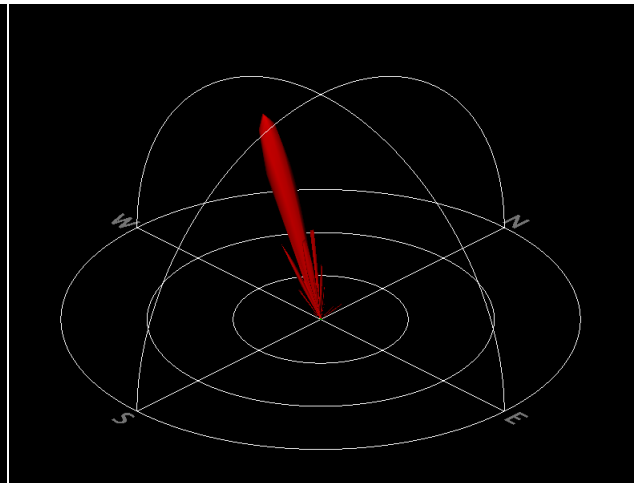
# Magnetic Zenith



2.70 MHz



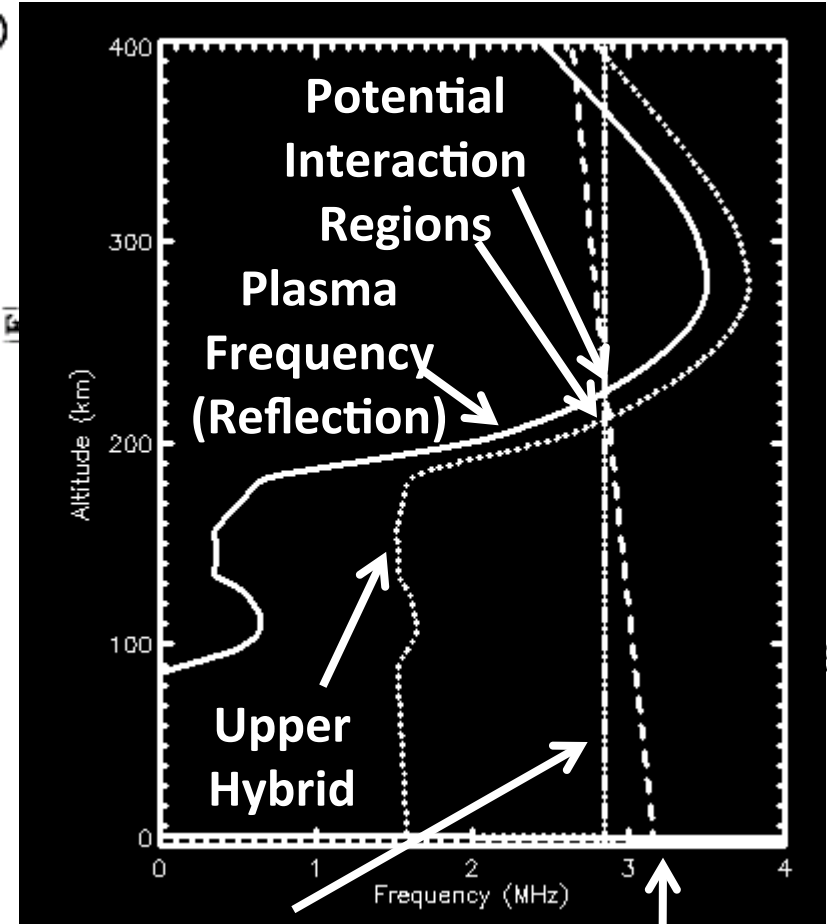
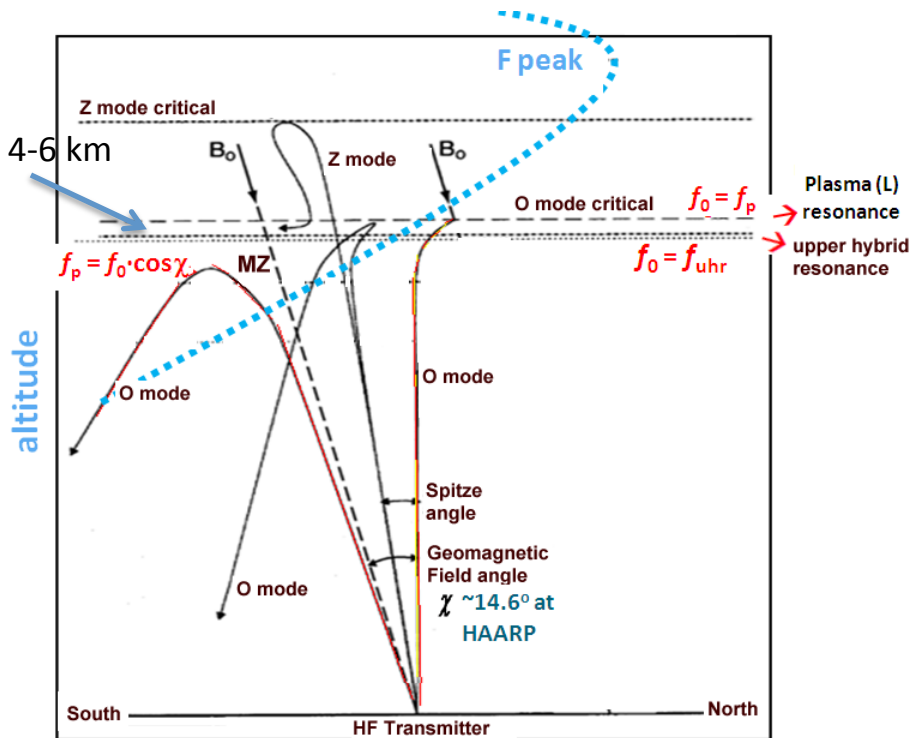
5.95 MHz



9.2 MHz

# HF PATHS – RESONANCE FREQUENCIES

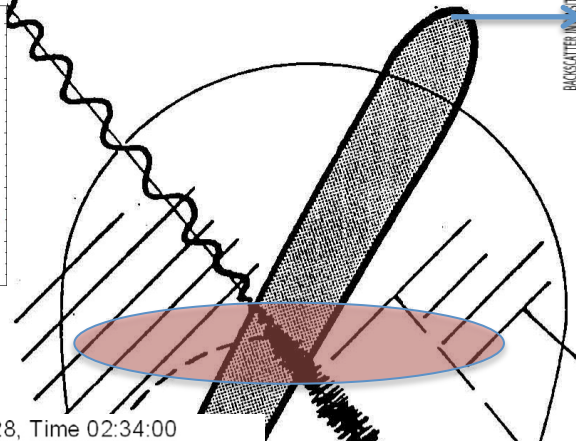
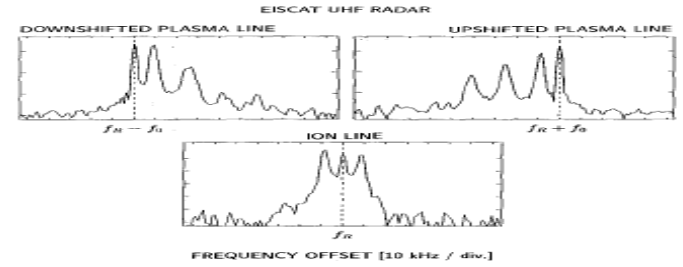
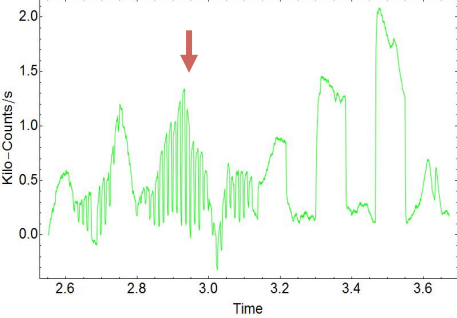
HF frequency equals; Plasma frequency, Upper hybrid, **double resonance** if upper hybrid coincides with cyclotron frequency



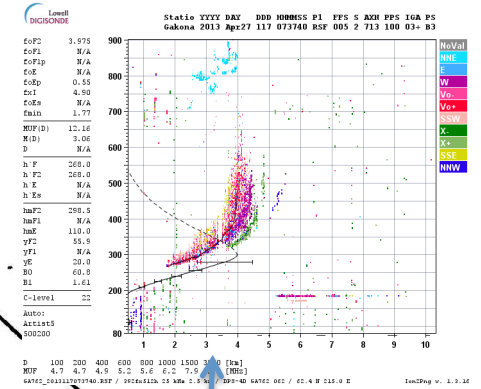
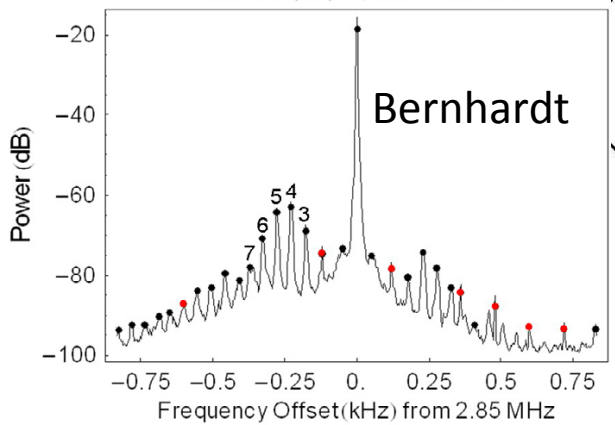
Transmitter Frequency      2<sup>nd</sup> Gyroharmonic



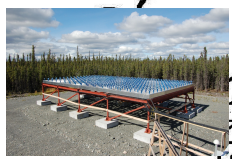
HAARP Photometer Channel 1, 2012 11 17



Date 2008/10/28, Time 02:34:00



HF RECEIVER



HAARP

SPECTROMETER



ASIP IMAGER



SCINTILLATION RCVR

HF DIGISONDE

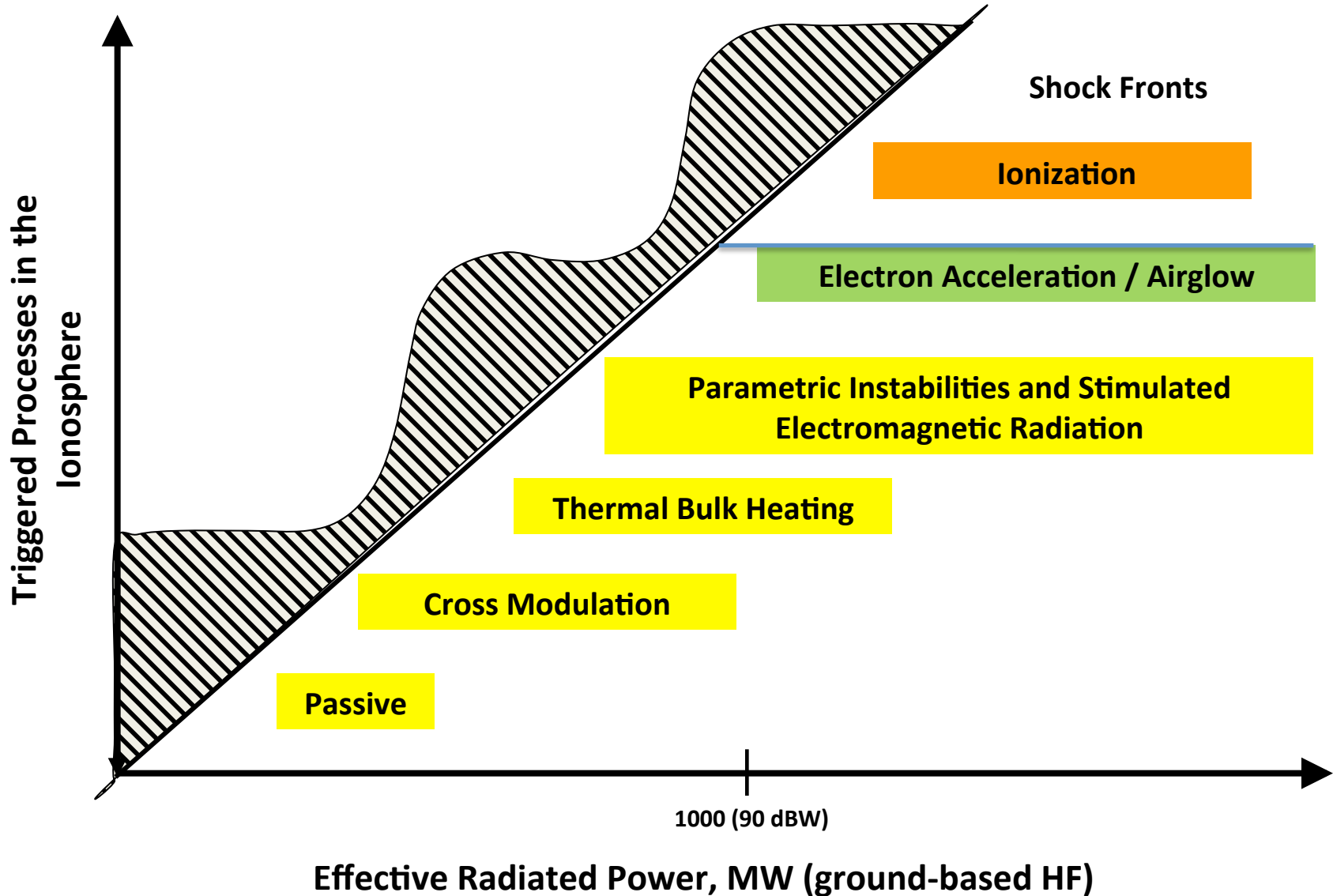
VHF BACKSCATTER

SEE

PHOTOMETER



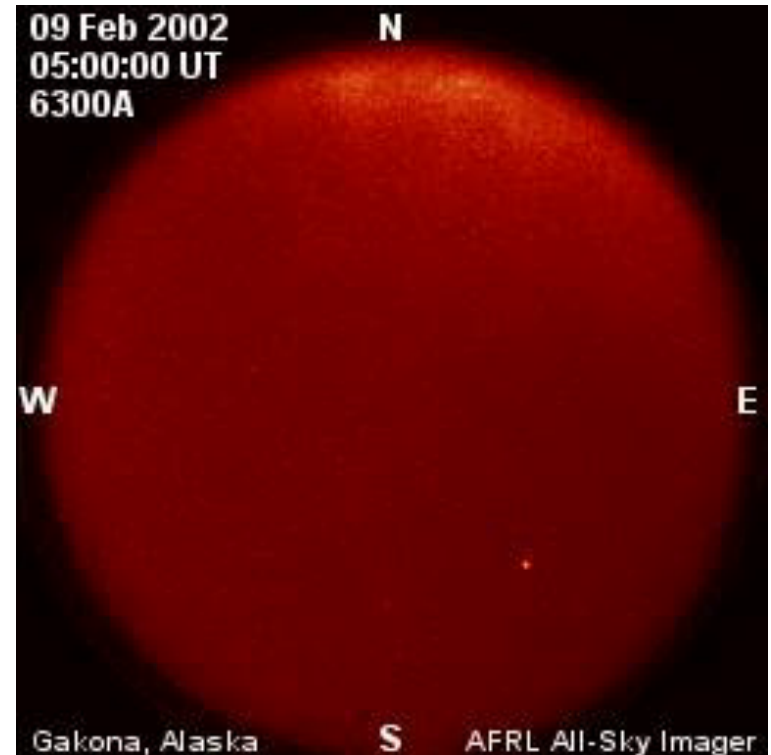
# Power Thresholds to Trigger Processes in the Ionosphere





# Artificial Aurora – The Zenith Effect

## Electron Acceleration (HAARP at 1 MW, EISCAT)

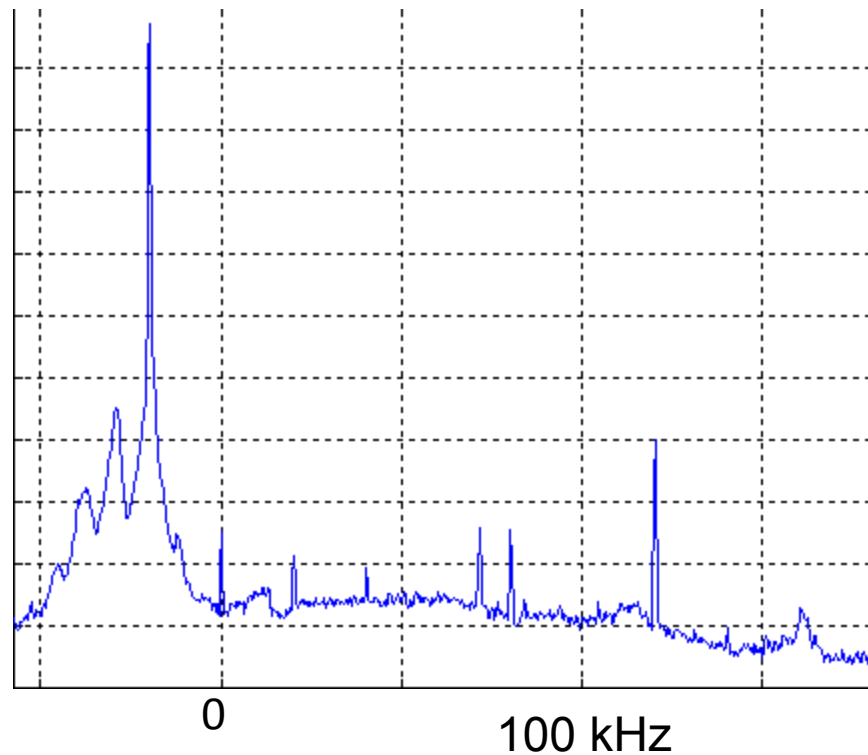




# SEE Gyro-Harmonics

## Sub-threshold Power

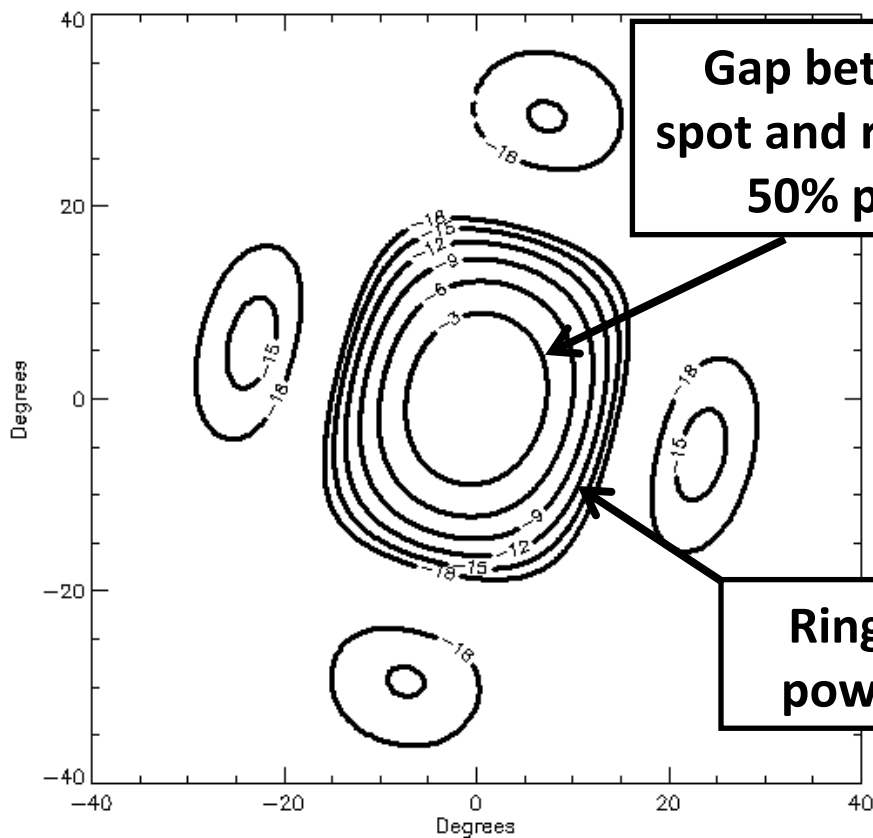
Double resonance near 4<sup>th</sup> cyclotron harmonic- HF frequency at zero shift 5.4 MHz



## HAARP AT 3.6 MW – NEW THRESHOLD - APL

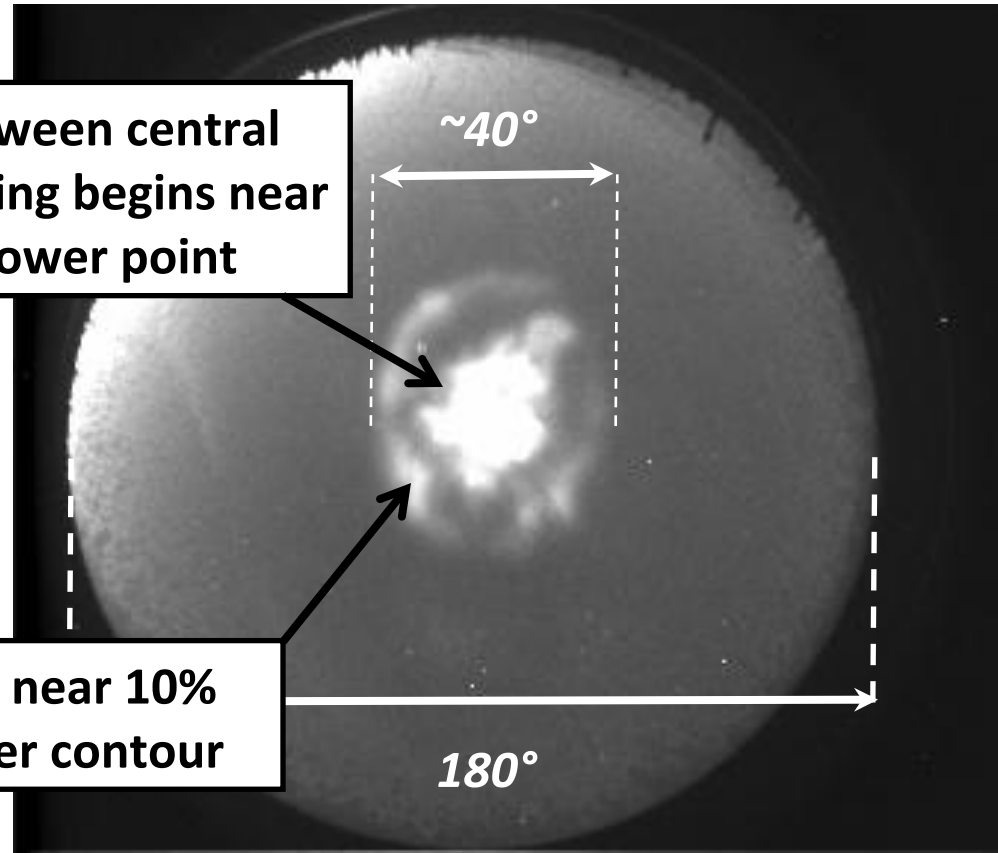
- First science experiments at full power showed unexplained spot-within-ring, bull's-eye patterns in optical emissions extending beyond beam edges filling  $\sim\frac{1}{4}$  of sky. Pedersen et al. GRL, 2009

### HAARP Transmitter Beam Pattern



Gap between central spot and ring begins near 50% power point

Ring near 10% power contour

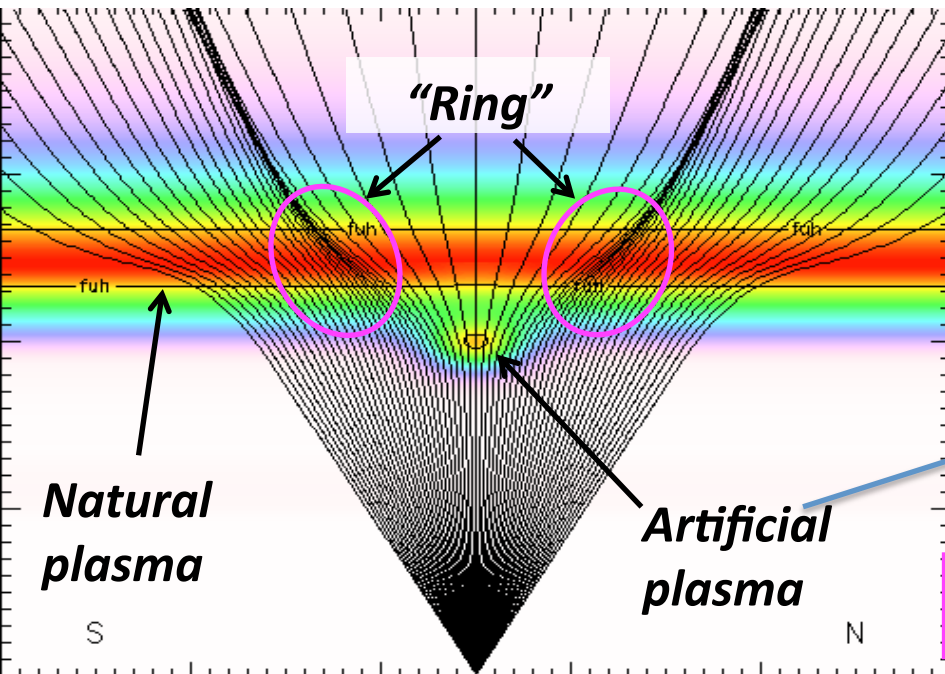


Non-Linear Reality at 3600 kW



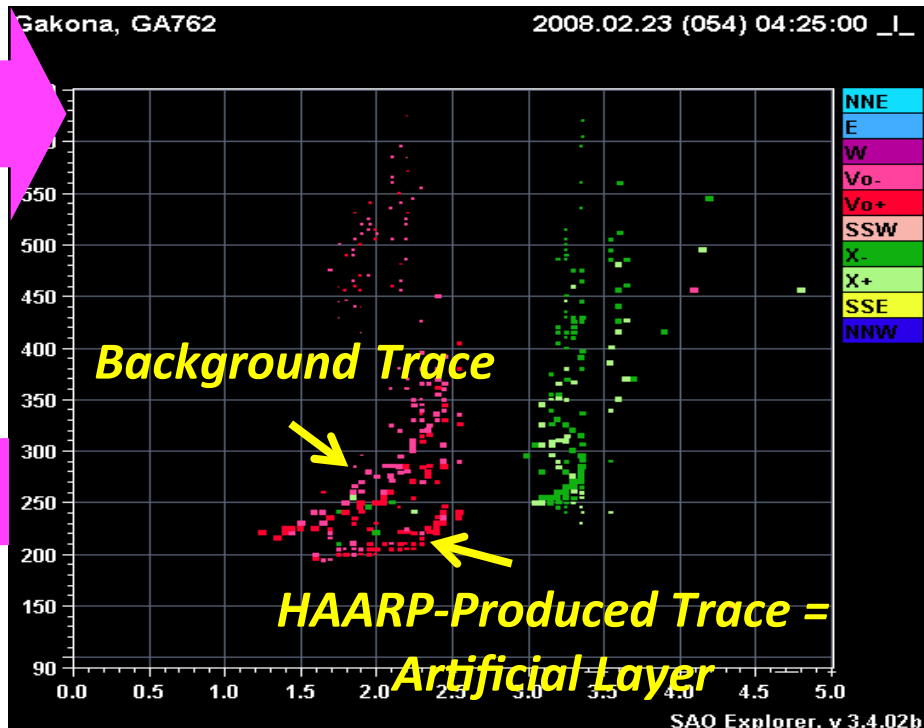
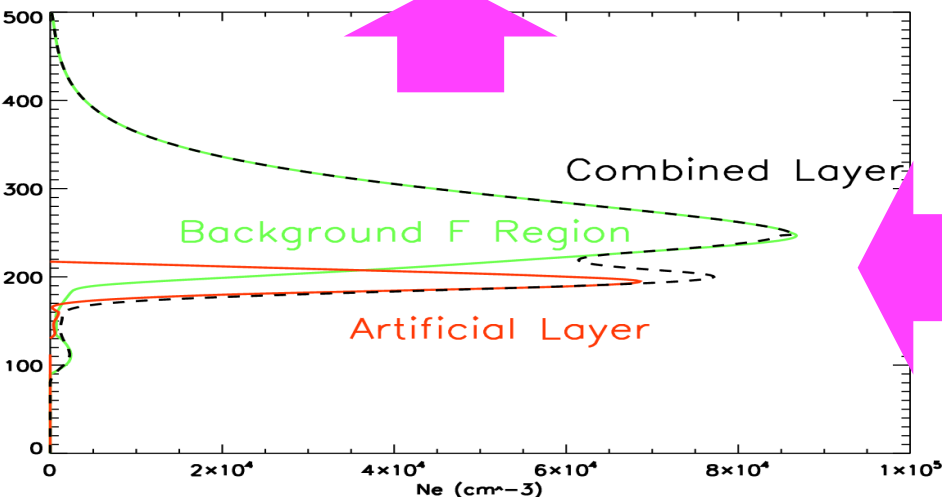
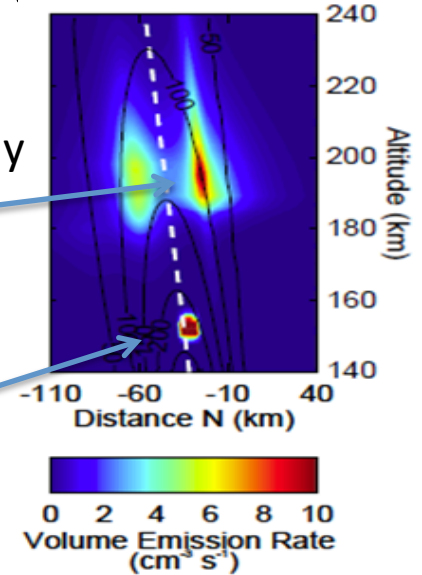
# HYPOTHESIS – ARTIFICIAL PLASMA LAYER

PEDERSEN ET AL, GRL 2009,2010,2011



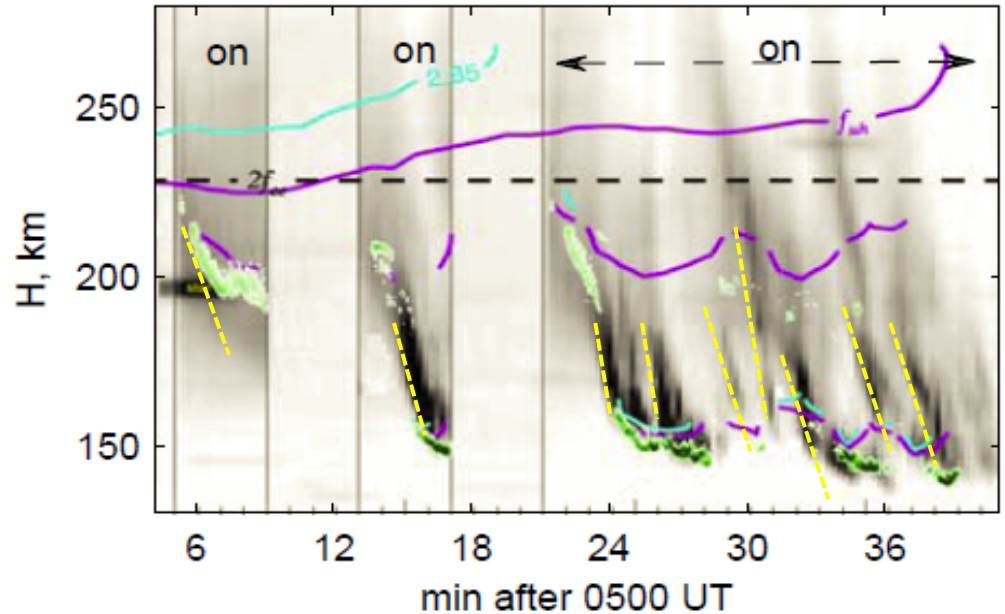
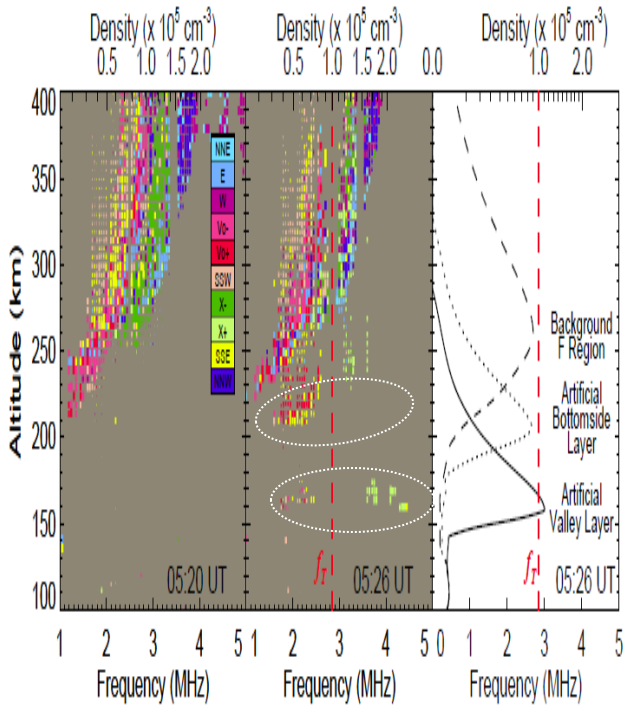
Cartoon

Tomography  
Reflection



# Descending APL

2GH, 440 MW, MZ



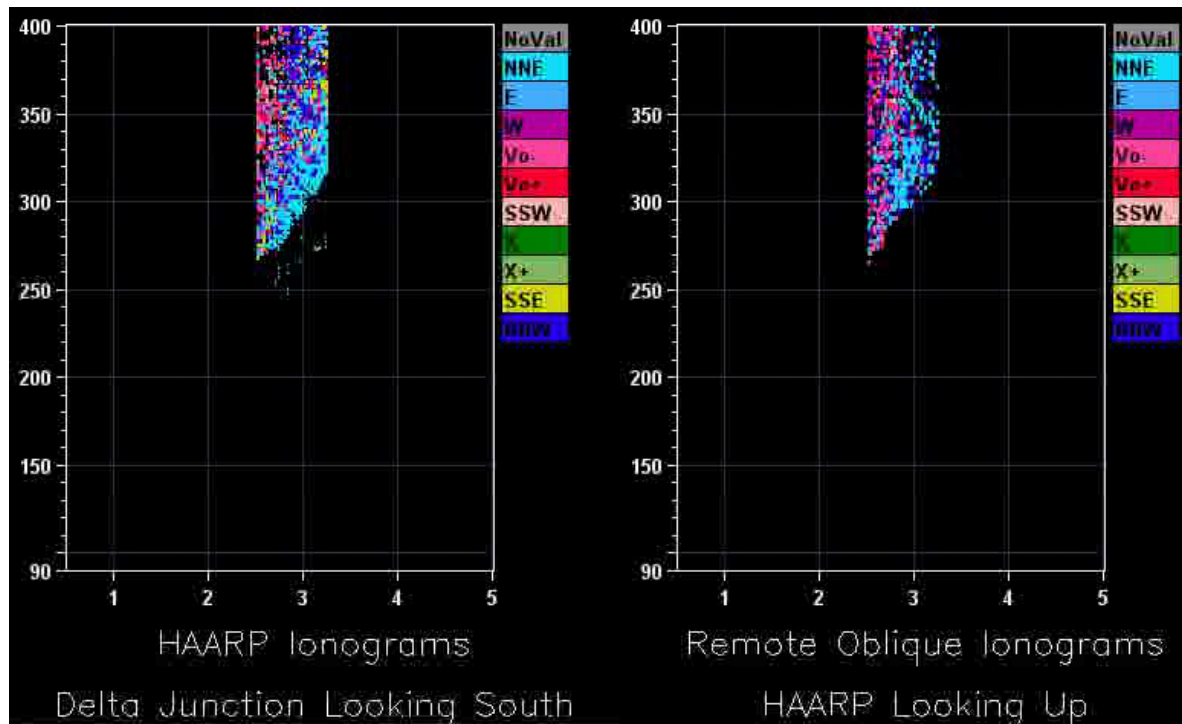
- (left) Background echoes (the heater off).
- (center) Heater on: Two lower layers of echoes near 160 and 200 km virtual height for 210 s.
- (right) True height profiles.

Time-vs-altitude plot of 557.7 nm optical emissions along  $B$  with contours showing the altitudes where  $f_p = 2.85$  MHz (blue),  $UHR = 2.85$  MHz (violet), and  $2f_{ce} = 2.85$  MHz (dashed white). Horizontal blips are stars. Green is the Ion Acoustic Line intensity.  
 ✓ the artificial plasma near  $h_{min}$  was quenched several times.



# Multi-Site Optical and Ionosonde Measurements During Frequency Ramp

- Simultaneous local and remote optical and ionosonde measurements
- Complicated 3-D structure clearly apparent
- Two descending layers observed
- Apparently correspond to spot and ring
- Gradually die out at low altitude



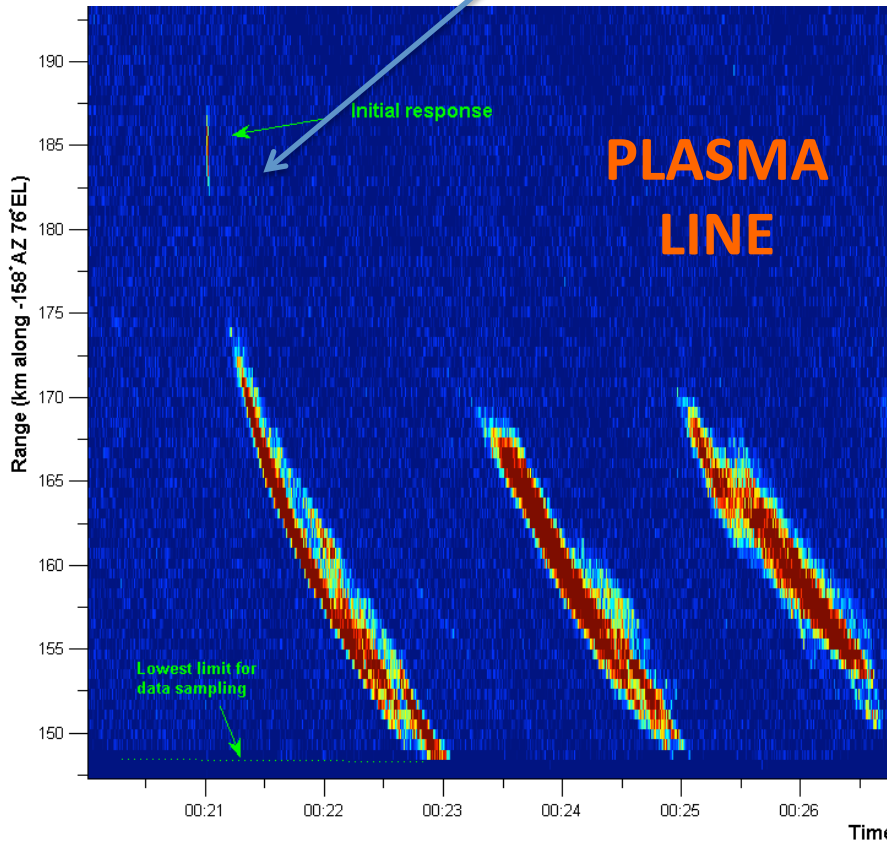
Courtesy of T. Pedersen

02:26:00 UT

2.850 MHz OFF



Note similarity with optical emissions descent except for initial response



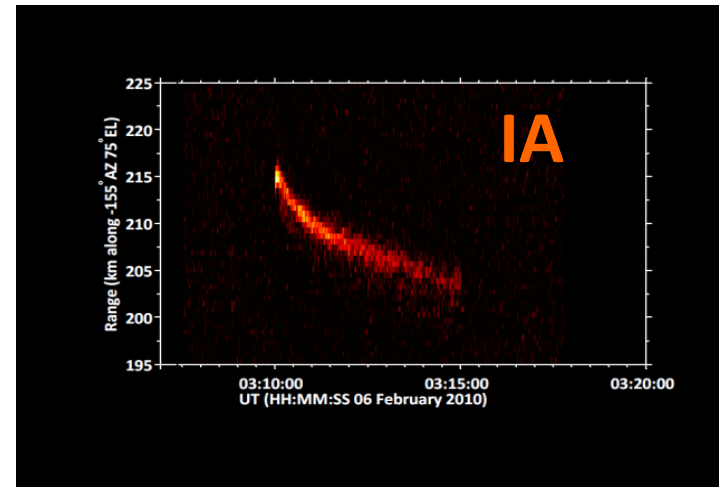
$$\Delta\omega \approx kC_s = 2k_o C_s$$

$$C_s = \sqrt{\frac{\gamma T_e}{M}}$$

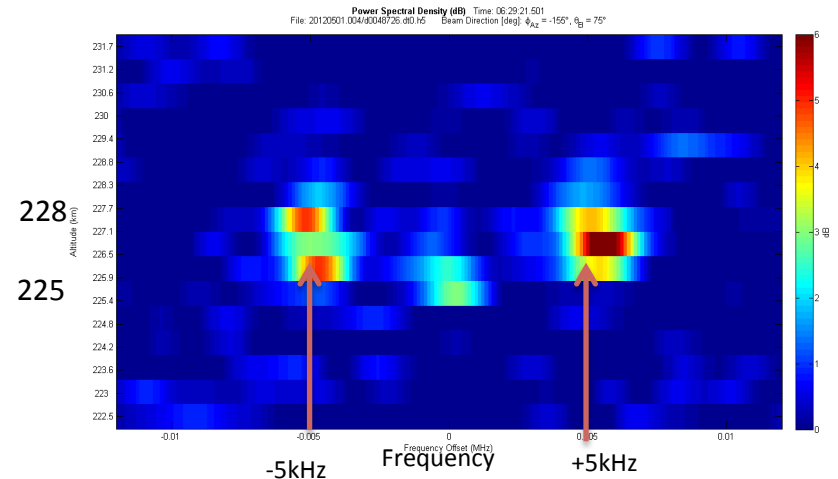
$$T_e \approx .65(M_{eff} / 20\gamma)(\Delta f / 5kHz)eV$$

## MUIR DATA - WATKINS frequency shift from 446 MHz

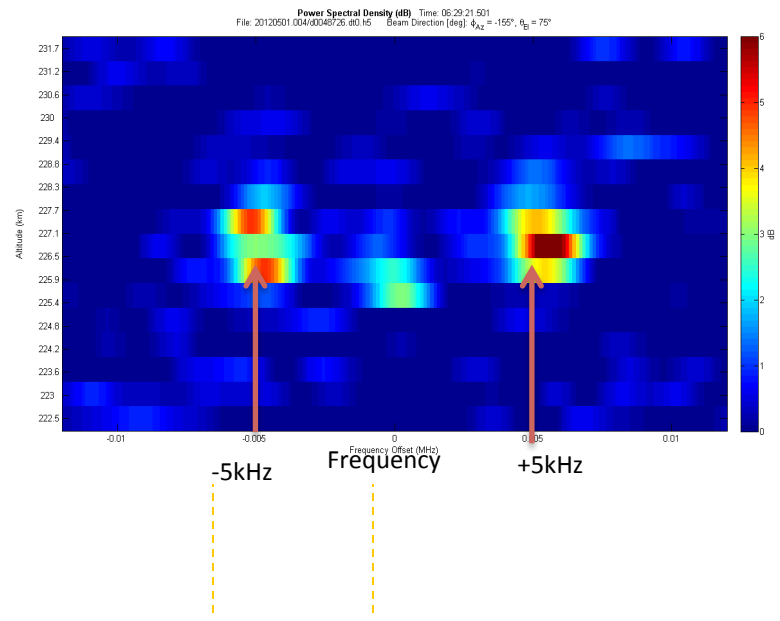
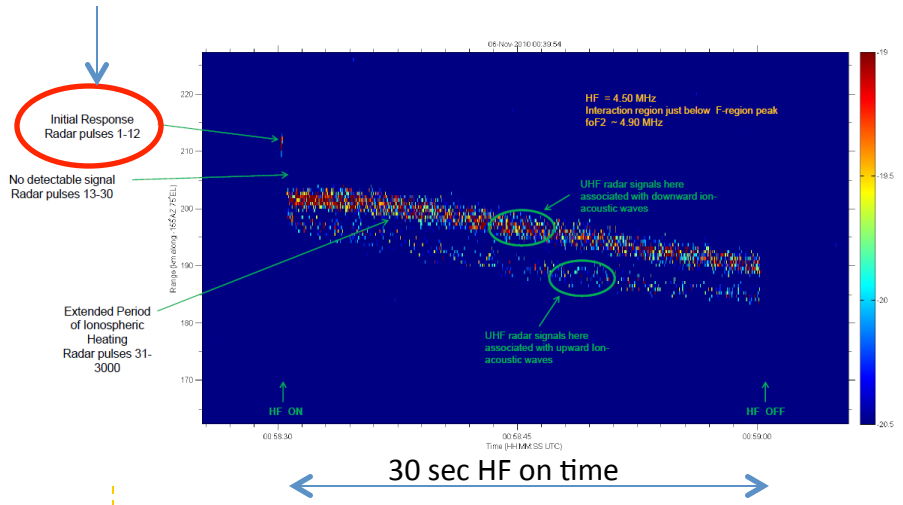
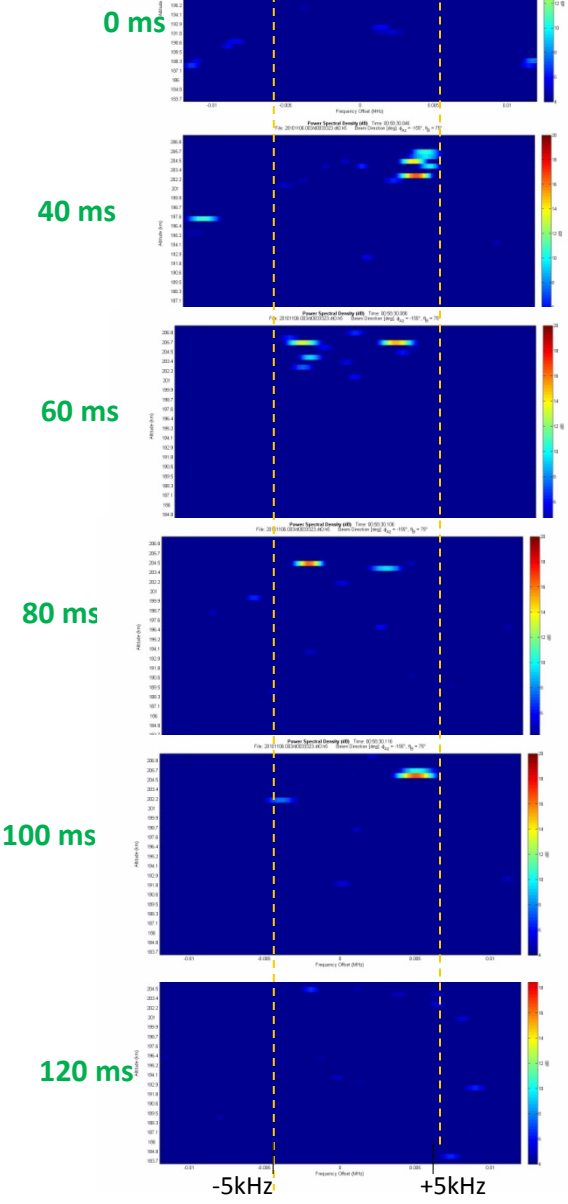
Example: UHF radar data showing downward progression of signals during 5 minutes of HF power



Descending ion-line and plasma line structures observed with UHF radar during heating.



# UHF Power Spectra During Initial Response Time (First 12 pulses after HF turn on - 120 milli-sec)



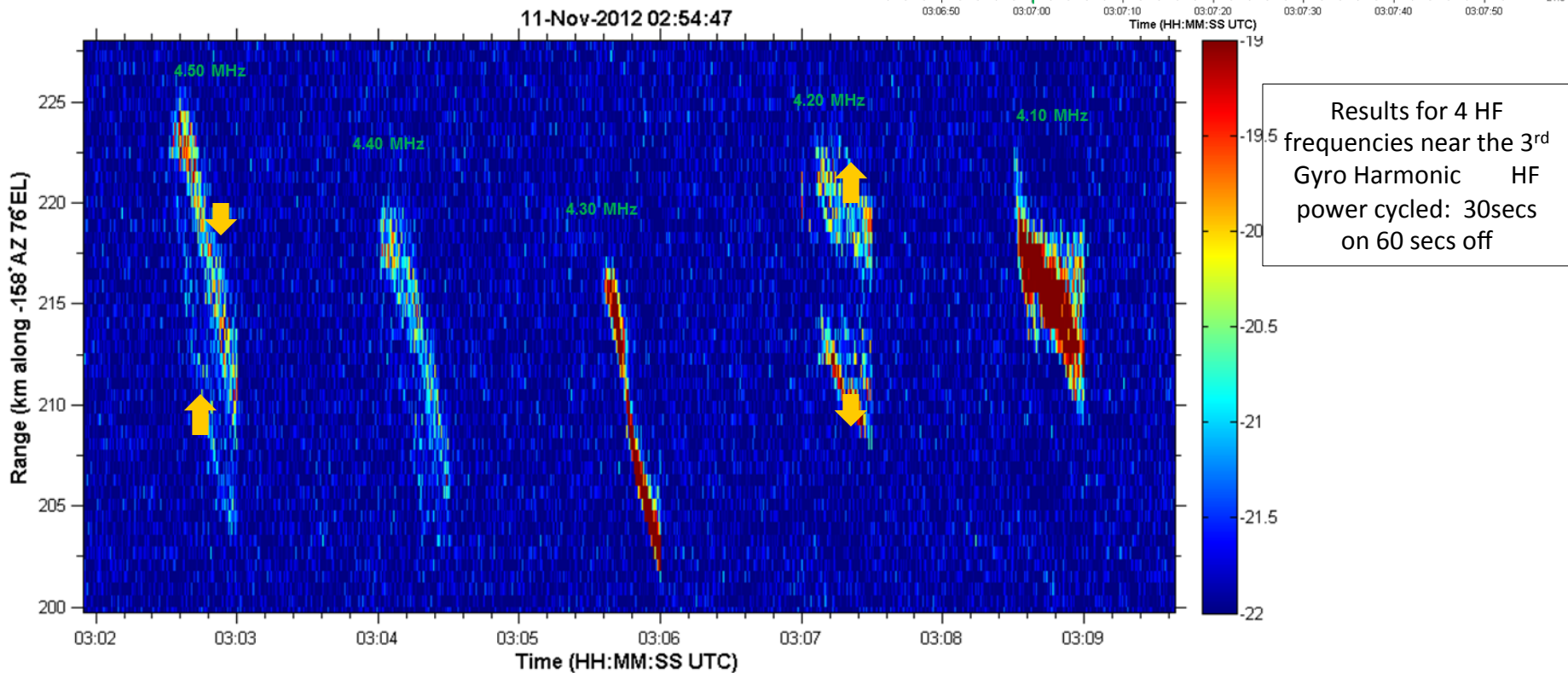
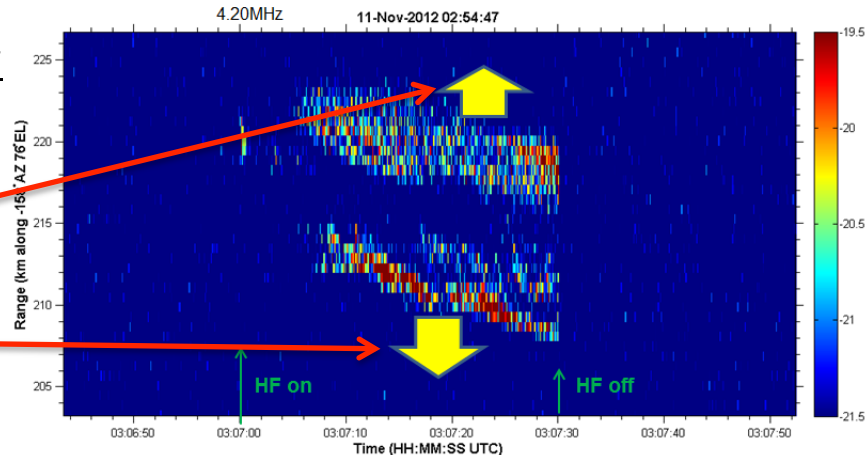
# UHF Radar Doppler Power Spectra Observations

Courtesy of B. Watkins

IA asymmetry ?

Upward

Downward



Results for 4 HF frequencies near the 3<sup>rd</sup> Gyro Harmonic HF power cycled: 30secs on 60 secs off

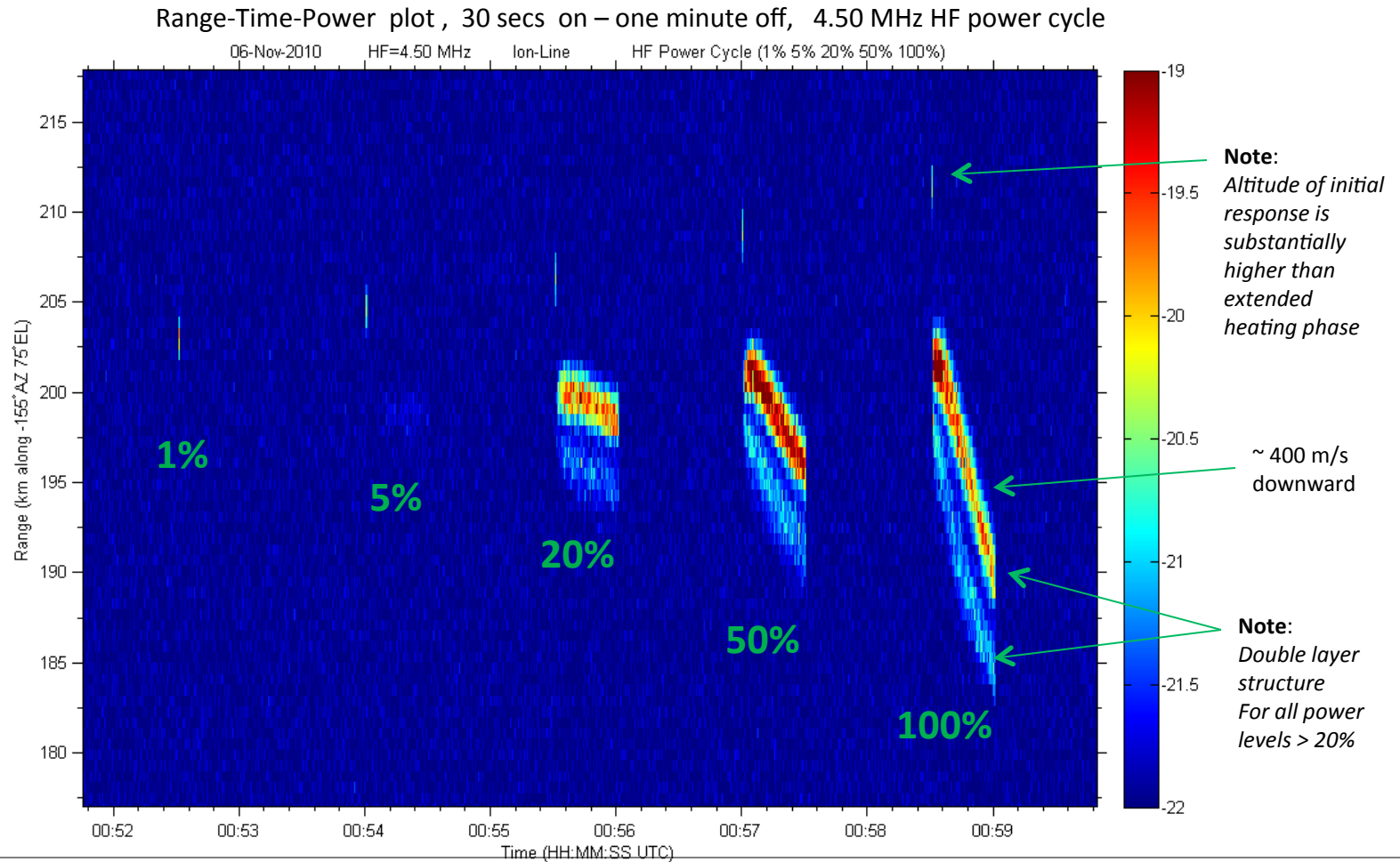
1. The 4.20 MHz frequency results show two distinct layers. (3<sup>rd</sup> gyro harmonic between 4.20 and 4.30 MHz)
2. Rate of descent approx same for 4.3, 4.4, 4.5 MHz. Lower descent rates for 4.1 and 4.2 MHz
3. Note direction of ion-acoustic waves for double layers that occur for 4.50 and 4.20 MHz. (yellow arrows)



# POWER THRESHOLD

Figure below: UHF radar scattering from HF-enhanced ion-line for HAARP power levels 1%, 5%, 20%, 50% 100% (3.6MW)

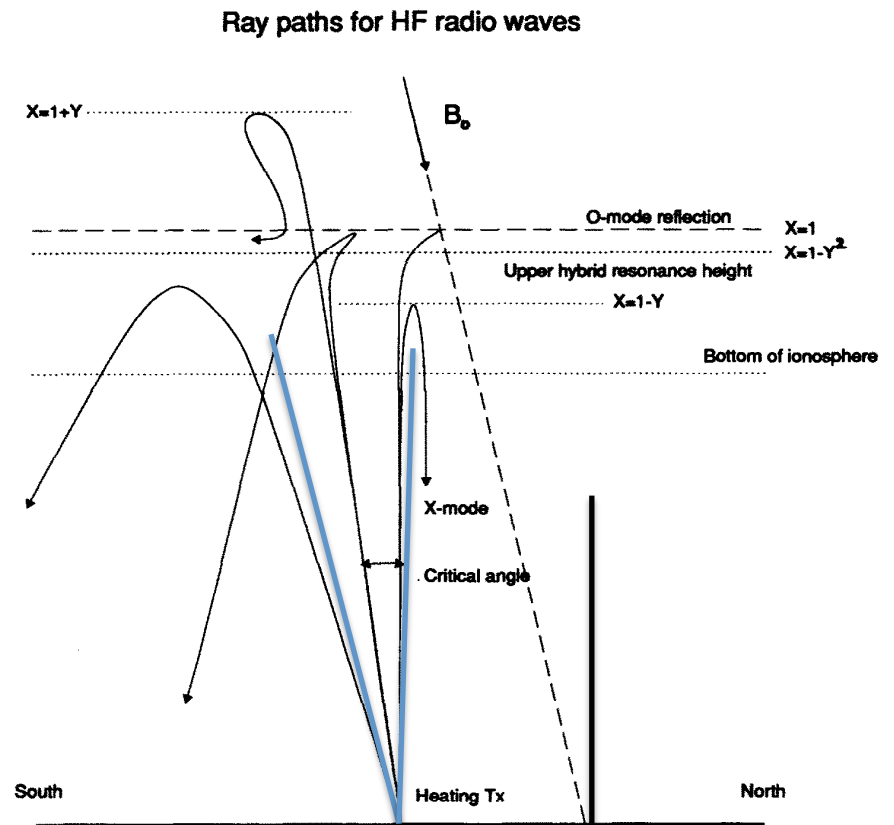
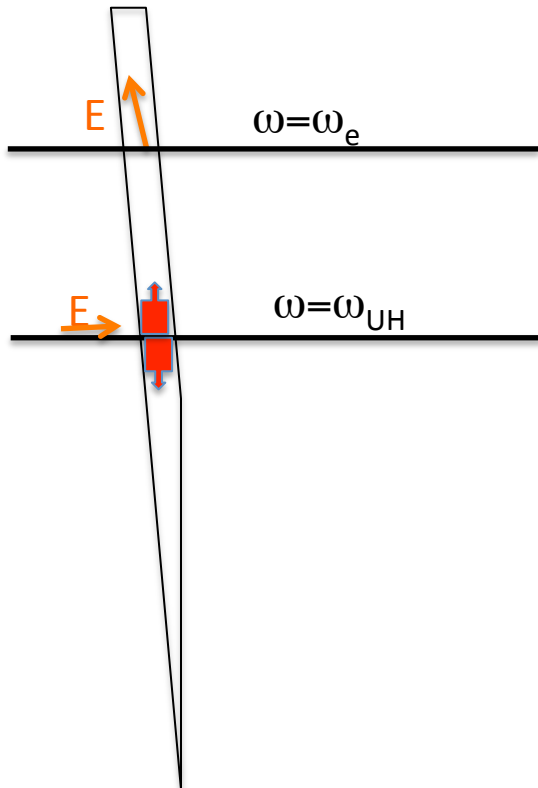
Downward progression of signals is indicative of large-scale heating.

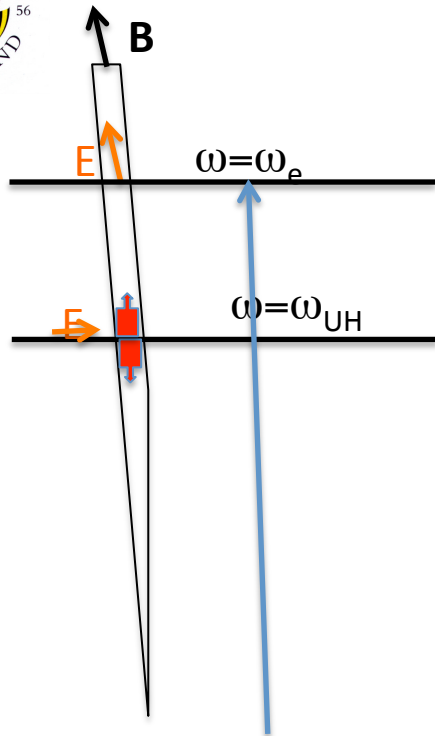


1. At least 20% of HAARP full power is required to attain substantial large-scale modification of ionospheric structure.
2. Double layer effect is not power-dependent. Exists for power greater than 20% level when signals are present.

## Theory/Modeling - Key Physics Ideas

- Electron acceleration controlled by Langmuir turbulence at the reflection height
- Electron heating controlled by upper hybrid heating including dual resonance
- Field aligned heat transport of heated plasma and energetic electrons





## Multi-time and length scale modular code (DAIL code suite- Eliasson et al. JGR 2012):

**Input:** (i) HF E at 100 or 150 km (ii) Ambient density (iii)  $T_e$

**Output:** (i) Temporal evolution of density (ii) optical emissions (iii) Supra-thermal EDF (iv) Plasma line

**Code Components:** (i) Multi-grid HF wave propagation with Zakharov eqs module (ii) Electron acceleration module using velocity diffusion tested against particle tracing (iii) Energetic electron transport model including elastic and inelastic collisions (iv) Ionization-recombination module (v) chemistry package (vi) optical emission package (vi) plasma wave package

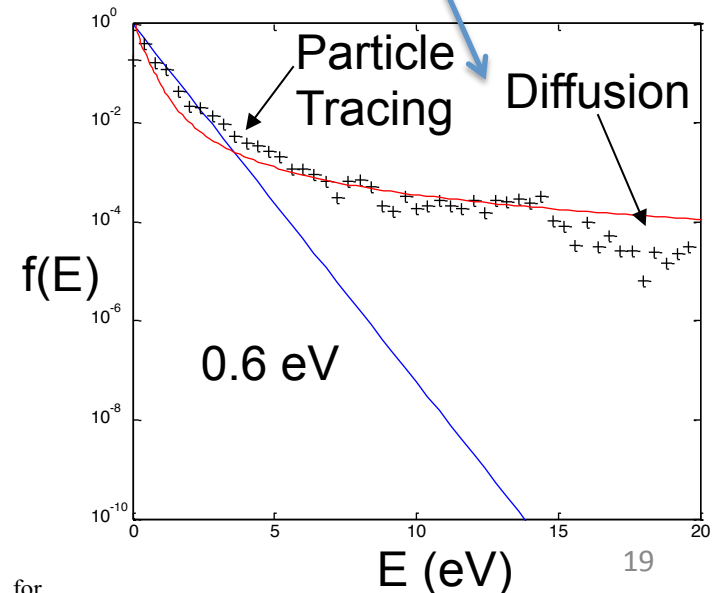
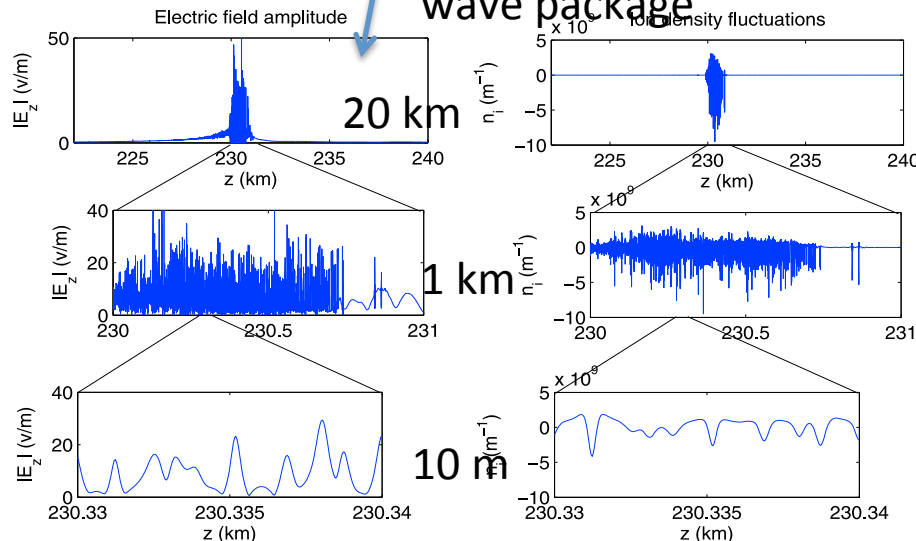
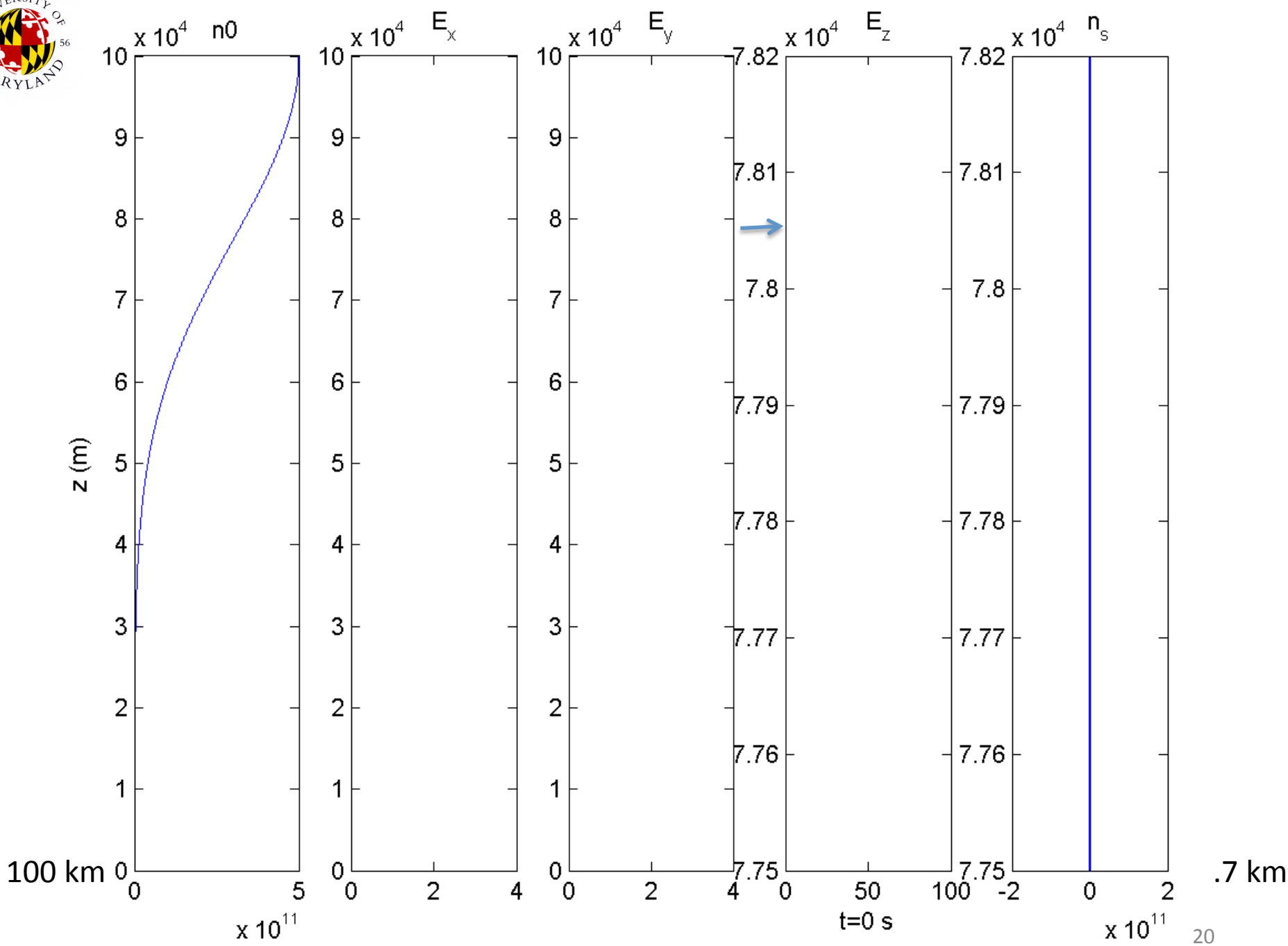
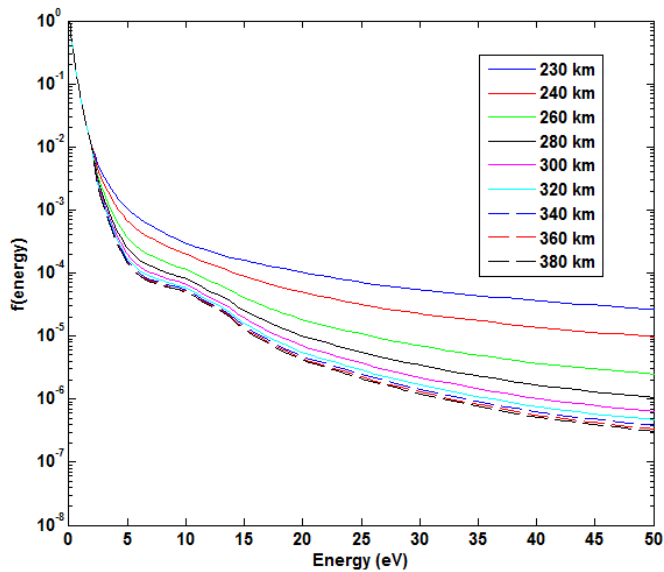
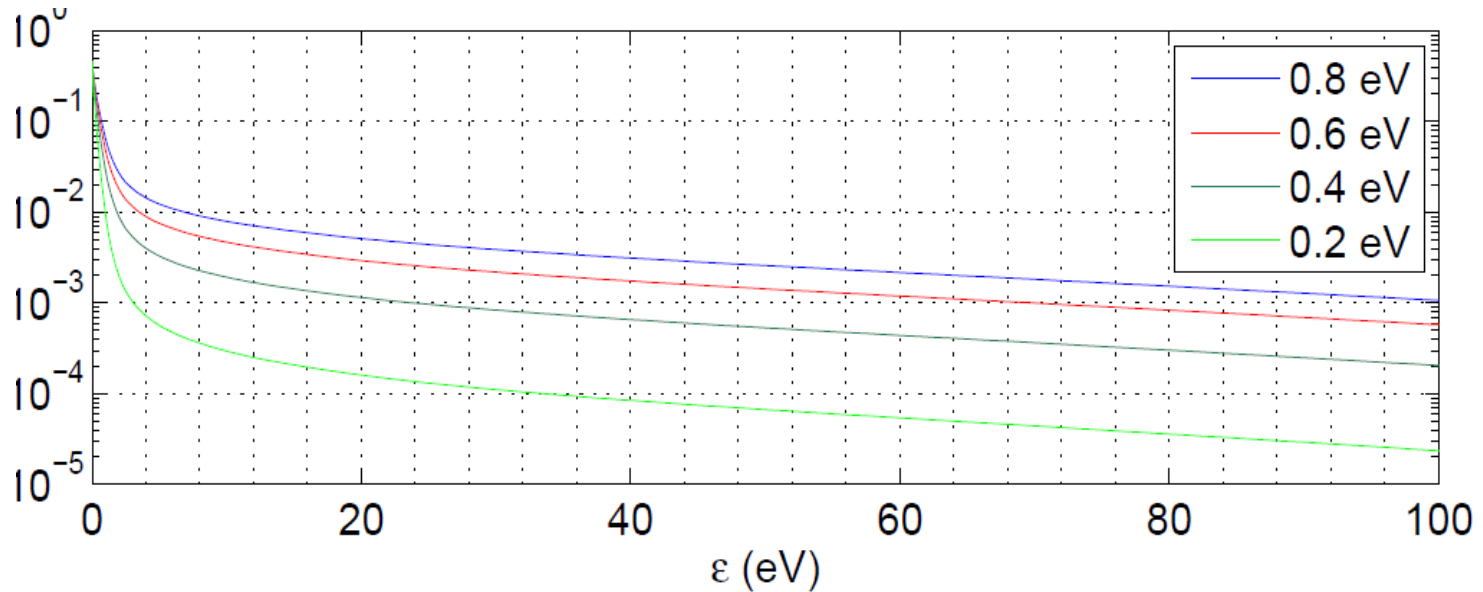


**Figure 2.** The amplitude of  $E_z$  and slowly varying ion density fluctuations  $n_i$  at various altitudes, for  $E_0 = 1.5V/m$ .

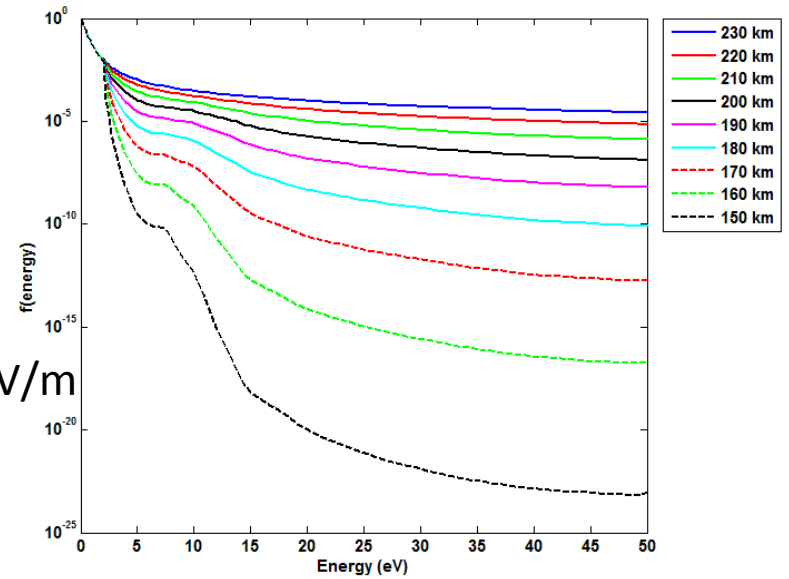




# Normalized EDF of supra-thermal electrons for E 1.5 V/m at 100 km

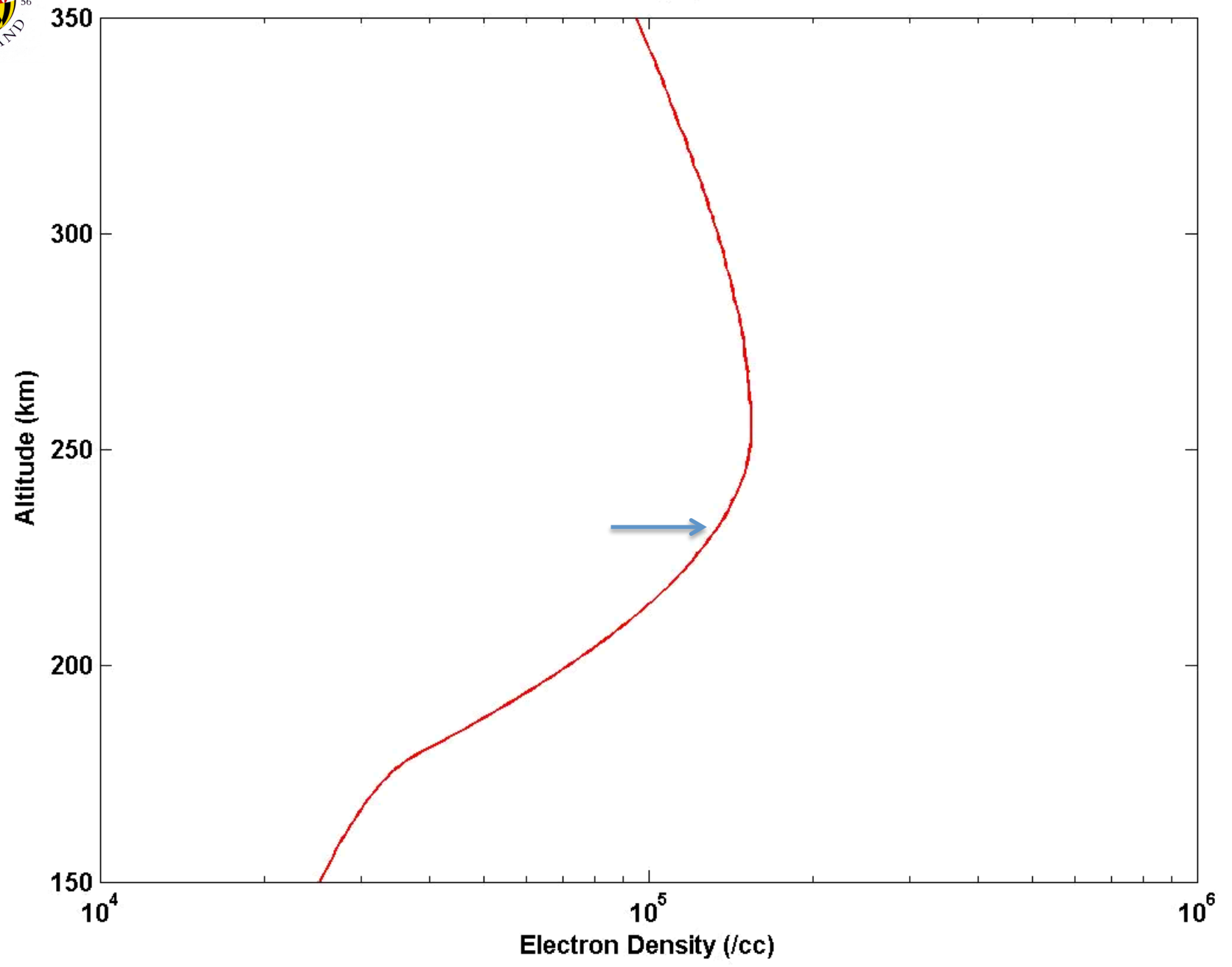


.6 eV, 1.5 V/m



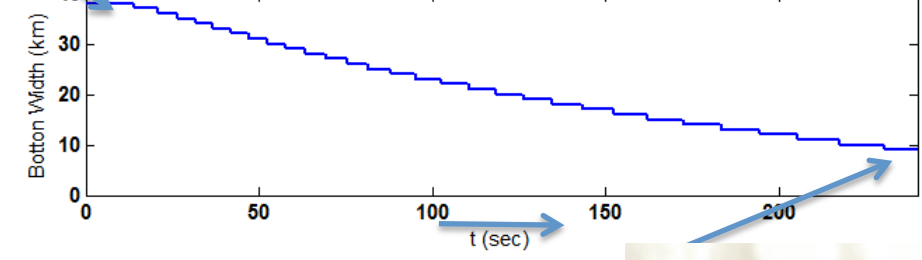
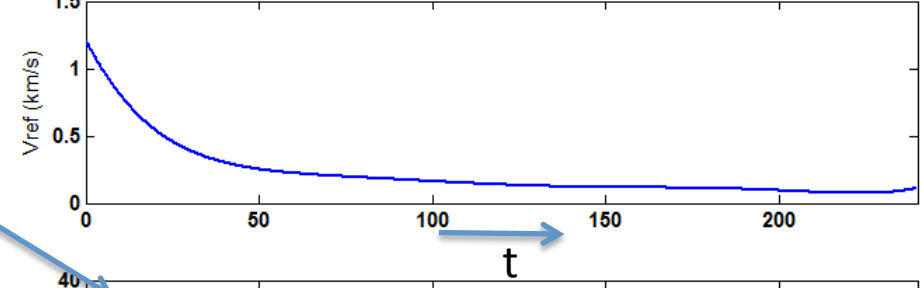
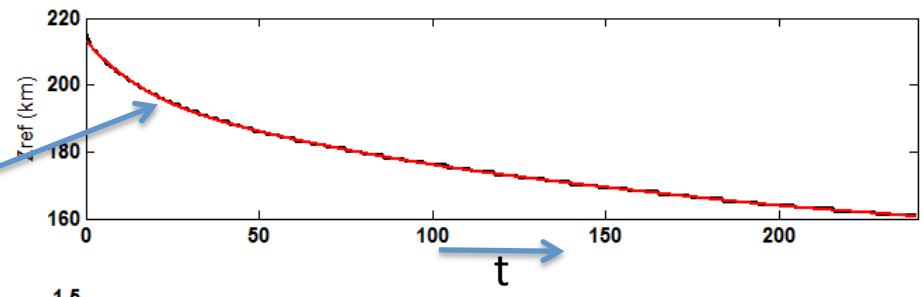
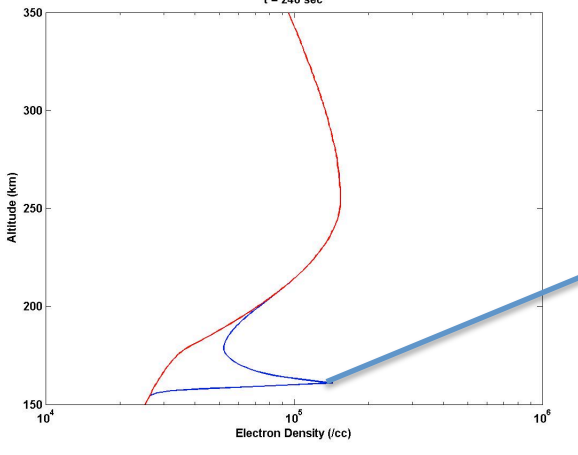
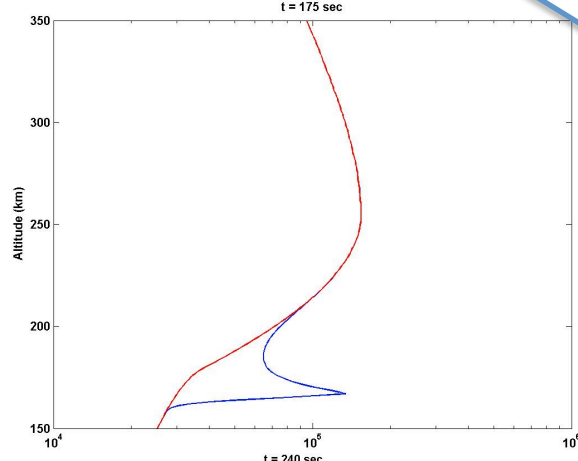
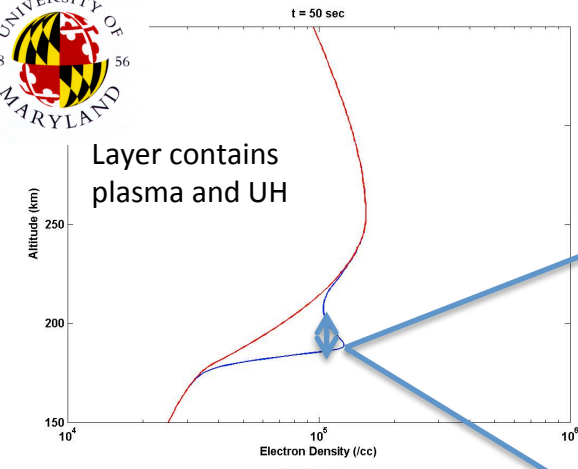


t = 2 sec

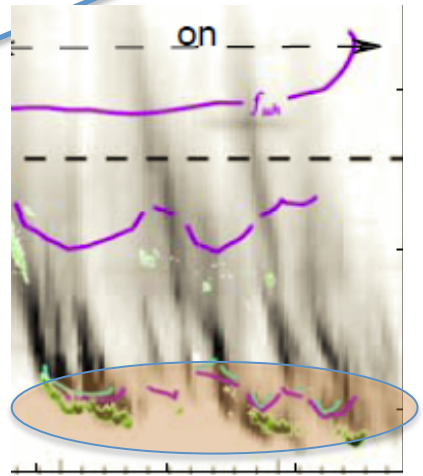




Layer contains plasma and UH



40 km  
10 km



Algorithm

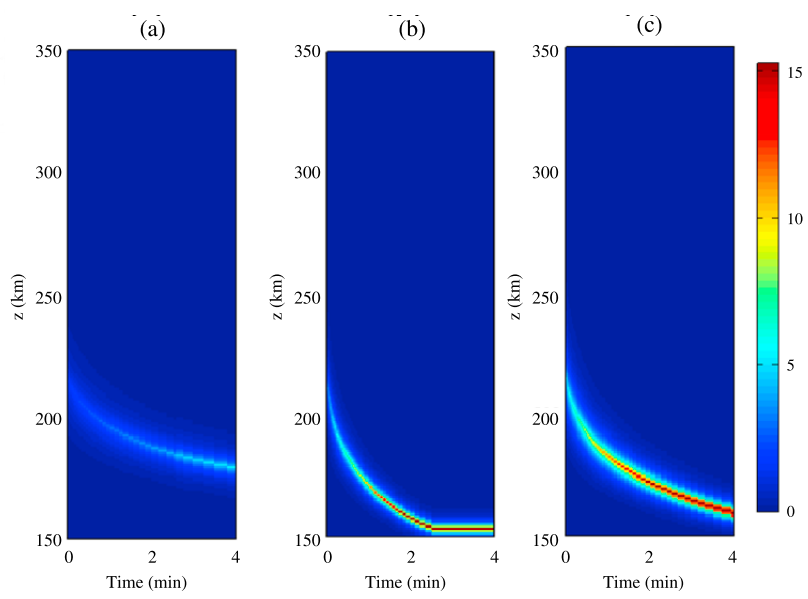
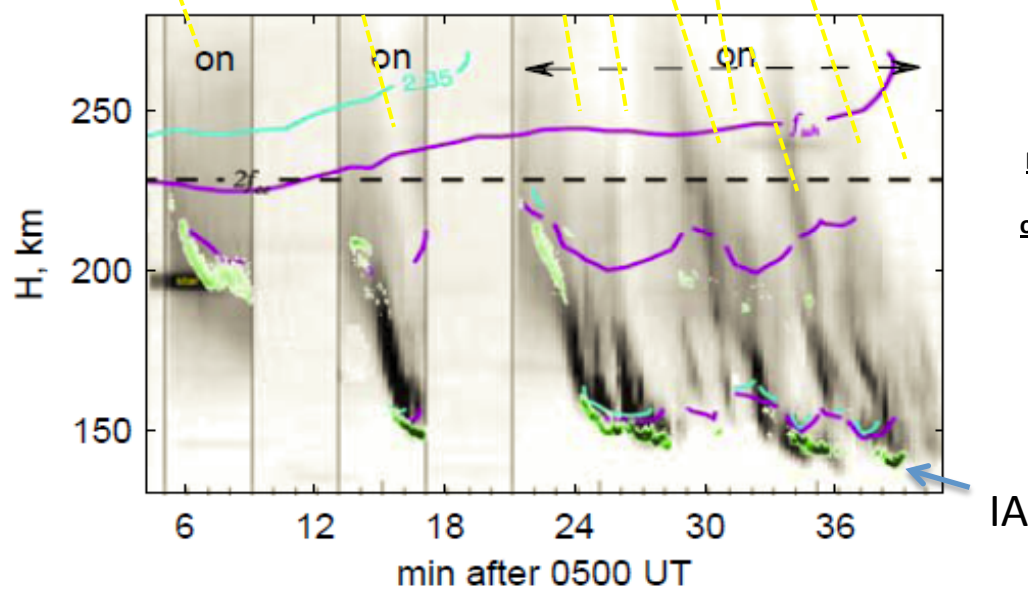
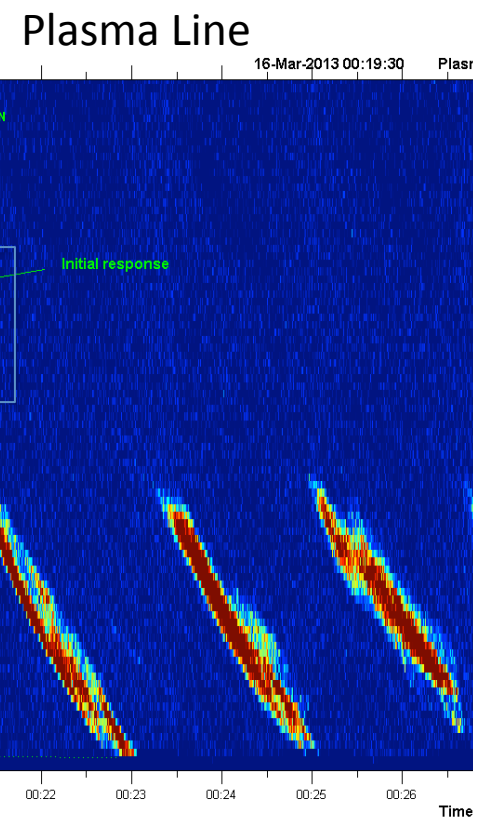


**Figure 13.** Green line emission as derived from simulation for different input wave amplitude and initial electron thermal energy: (a)  $E_0 = 1$  V/m,  $T_e = 0.4$  eV, (b)  $E_0 = 1.5$  V/m,  $T_e = 0.4$  eV, and (c)  $E_0 = 1$  V/m,  $T_e = 0.6$  eV.

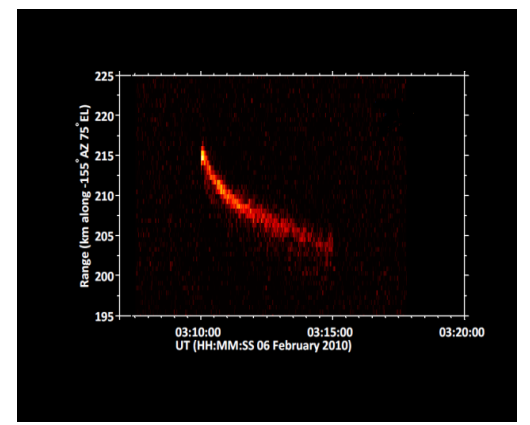


**Descending ion-line and plasma line structures observed with UHF radar during heating.**

Watkins

$f_p = 2.85$  MHz (blue),  $f_{UH} = 2.85$  (violet)

Pedersen et al. 2010

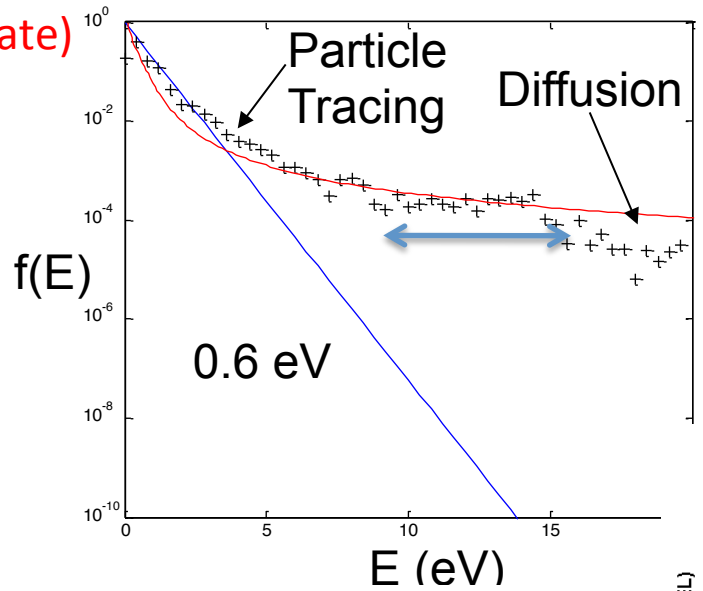
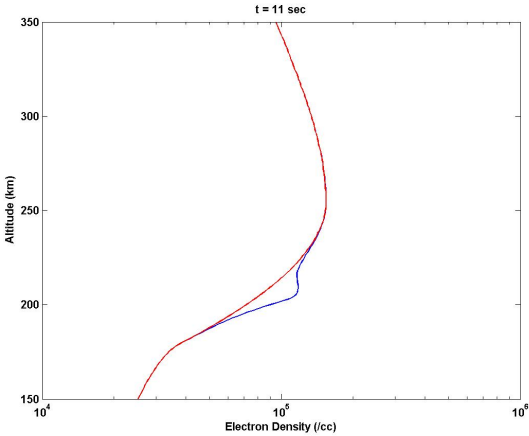


Ion Line





**HYPOTHESIS:** Hot plasma .4-.6 eV with **supra - thermal** tails creates enhanced IA and electron plasma waves **locally** –( IA and plasma waves are **damped within few meters and do not propagate**)

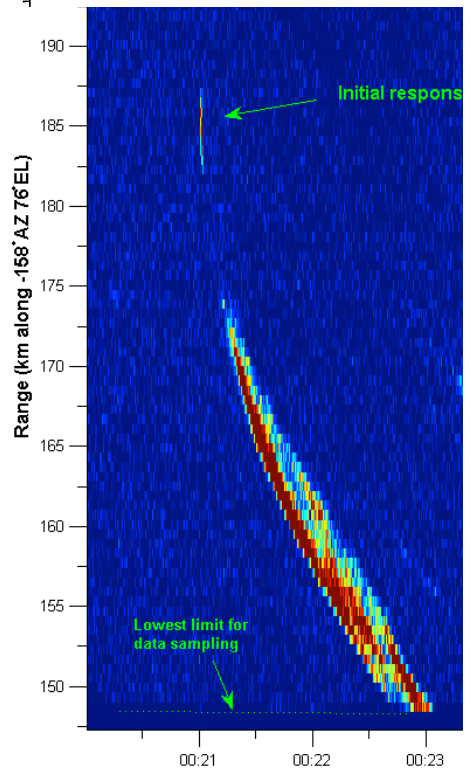
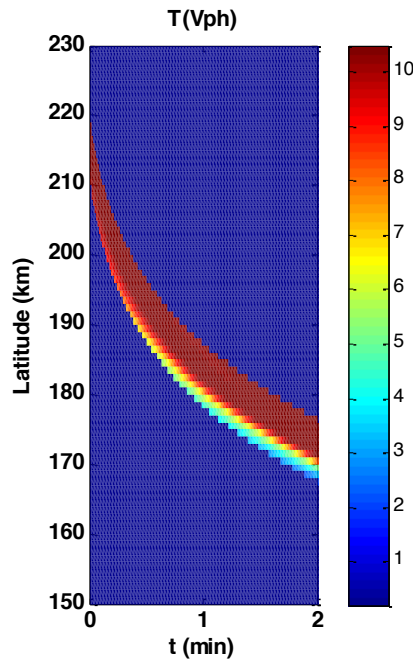


**Classic signature of hot plasma with supra-thermal tails**

$$\frac{\langle E^2 \rangle}{8\pi} \approx \frac{8ne^2}{\omega_e} \int_{k_1}^{k_2} dk k \frac{F_T(\omega_e / k)}{|F_T'(\omega_e / k)|}$$

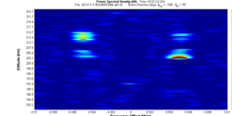
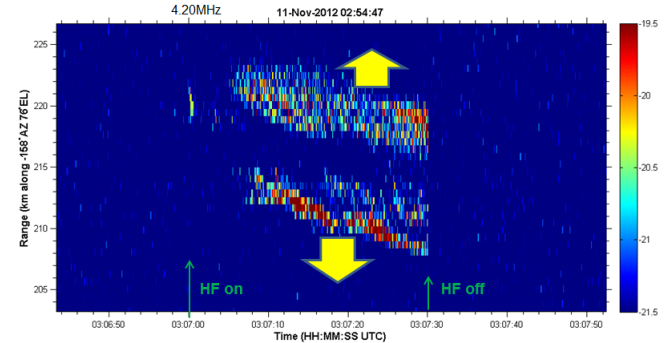
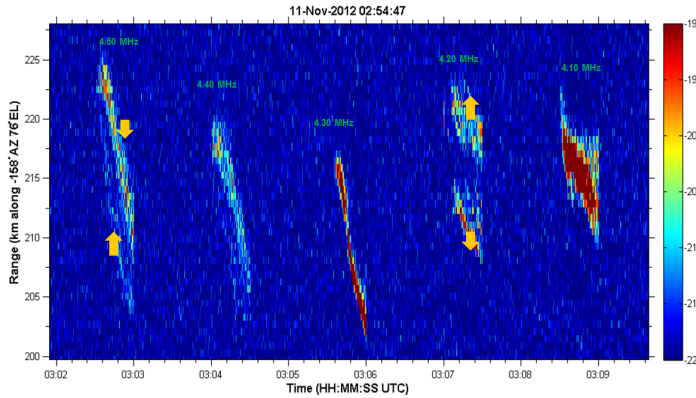
$$R < \frac{V_T^2 / V_e^2}{/n(V_E / \alpha V_e)} \rightarrow (\lambda_R / \lambda_D)^2$$

if  $v < \omega_e u_{ph}^2 F'(u_{ph})$



# ION LINE PECULIARITIES

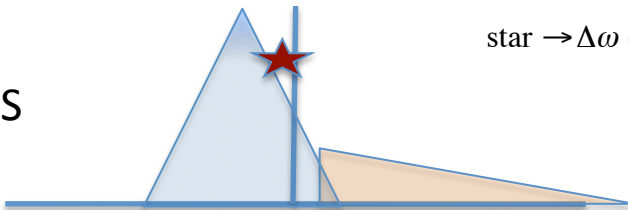
B. Watkins



Power-height-time plot of HF-enhanced ion-line signals. Close to 3<sup>rd</sup> gyro-harmonic signals split into two layers. Doppler spectra (example to left) show strong asymmetries that indicate mainly propagating only ion-acoustic waves in the upper layer. The downward layer is associated with primarily downward propagating ion-acoustic waves.

The above spectral asymmetries are interpreted to be the result of electron flow upward and downward from the HF interaction region as indicated by the yellow-colored arrows.

INJECTION  
DOWNWARDS

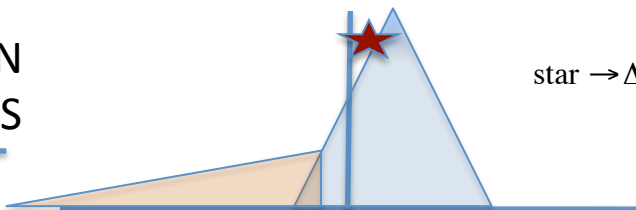


$$\text{star} \rightarrow \Delta\omega \approx 2k_R c_s$$

Plasma with drift  
 $\gamma(k)=0$  gives

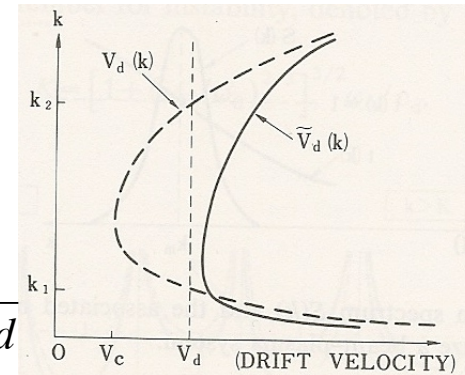
$$V_d(k) = (\omega_k / k) + (\text{ion L damping})$$

INJECTION  
UPWARDS



$$\text{star} \rightarrow \Delta\omega \approx -2k_R c_s$$

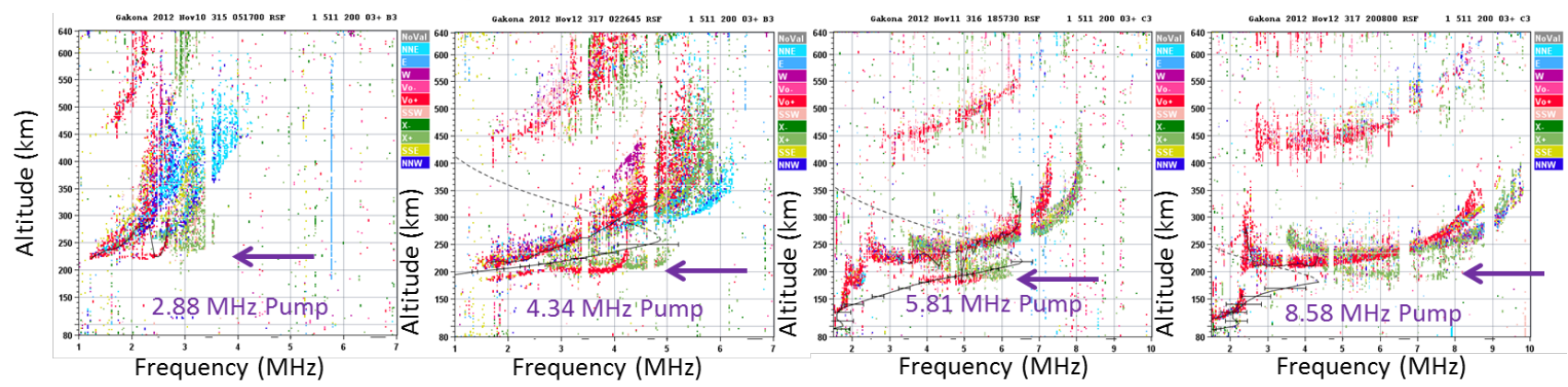
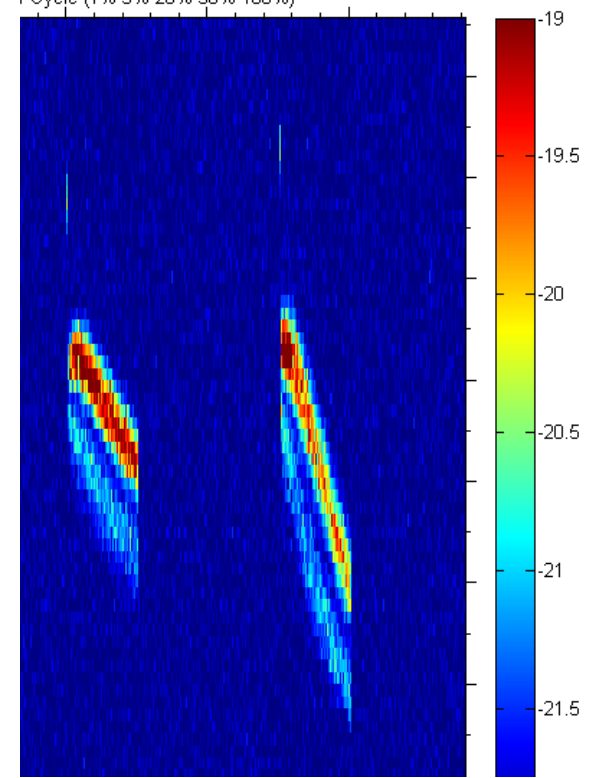
$$S(k) = \frac{1}{2} \frac{\omega_k / k}{V_d(k) - V_d}$$



# ONGOING PHYSICS STUDIES FOR INPUT TO DIAL MODEL

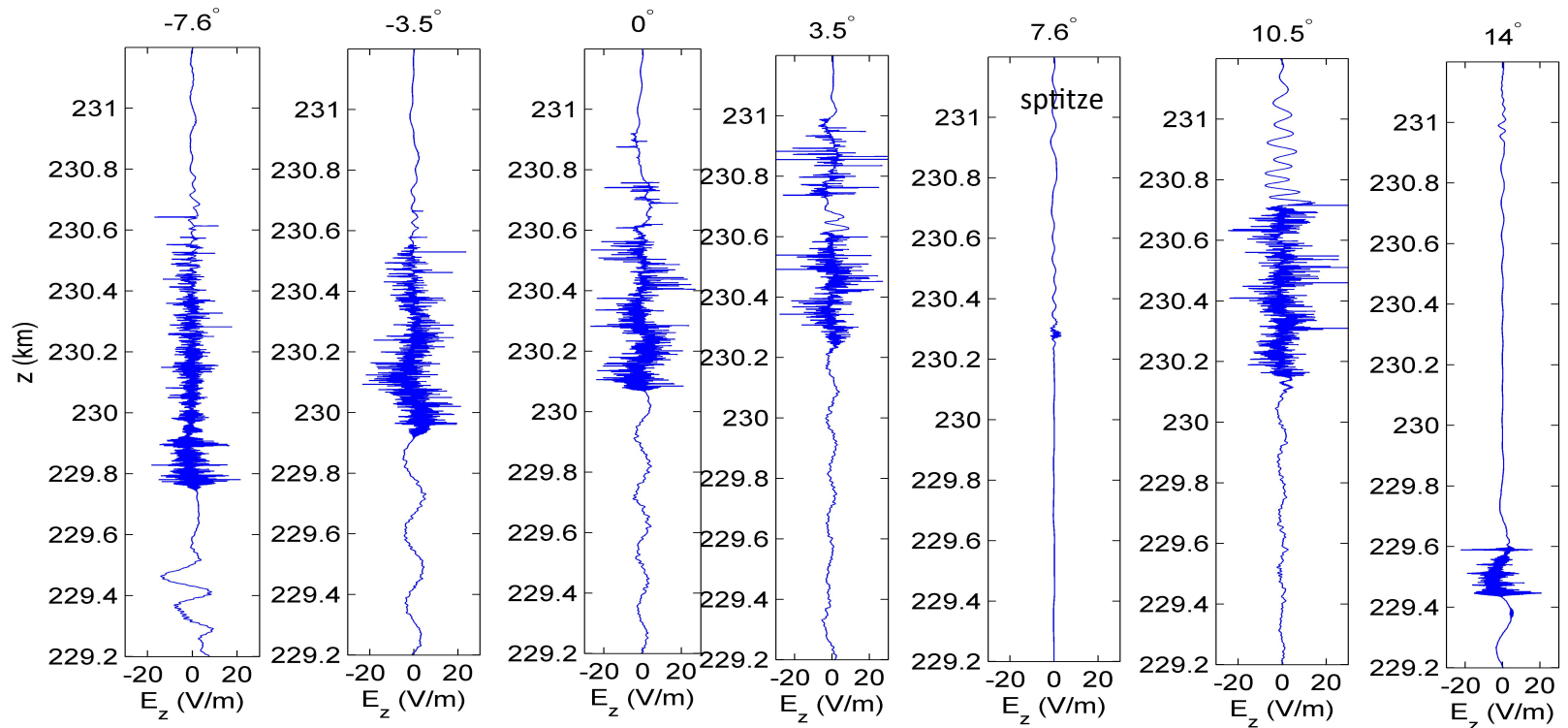
1. MULTI-DIMENSIONAL ISSUES
2. UPPER HYBRID
3. DOUBLE RESONANCE HEATING

P. BERNHARDT

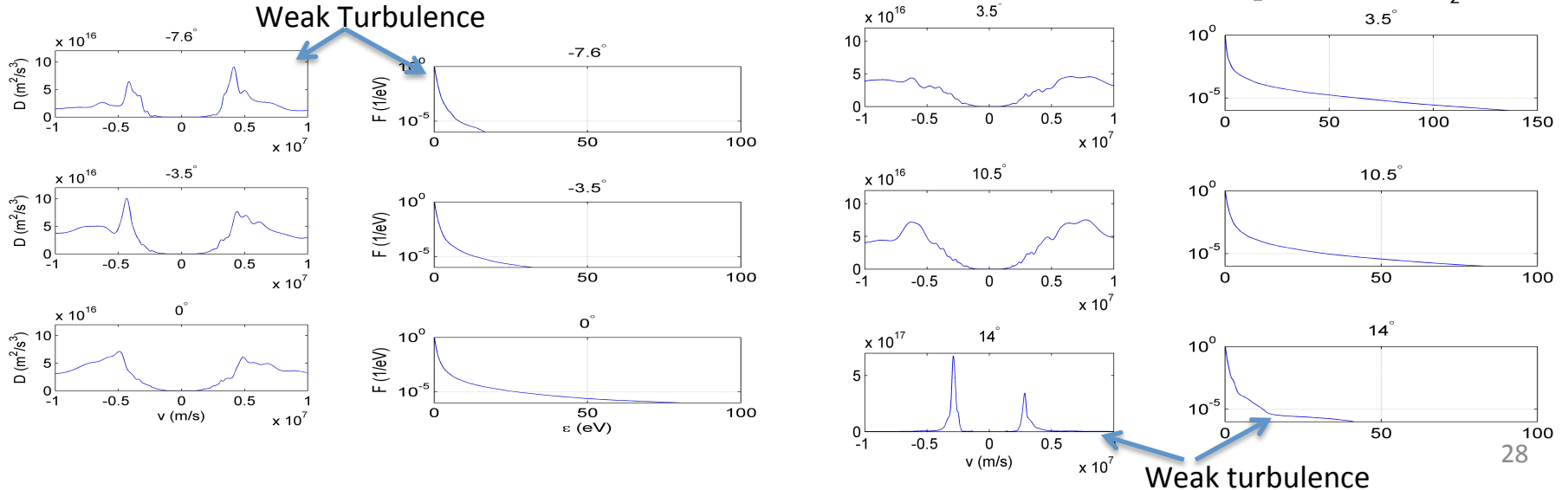




# O-mode, 1V/m amplitude, electron temperature 0.4 eV, and different angles of incidence,

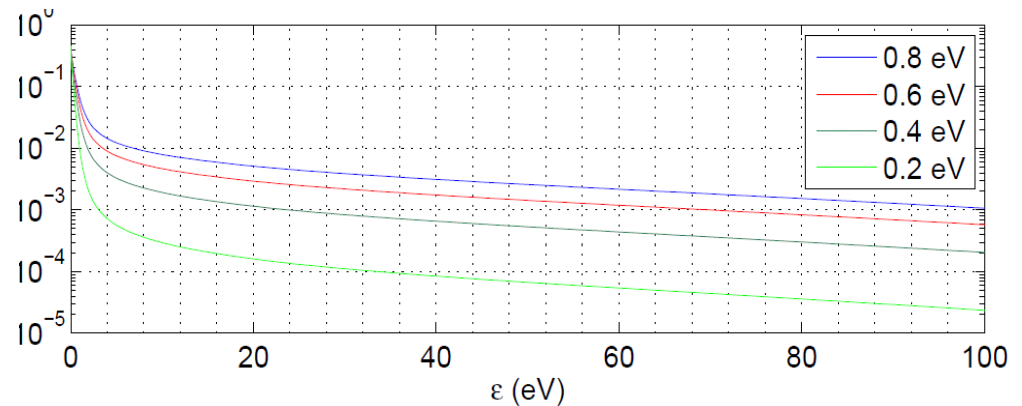
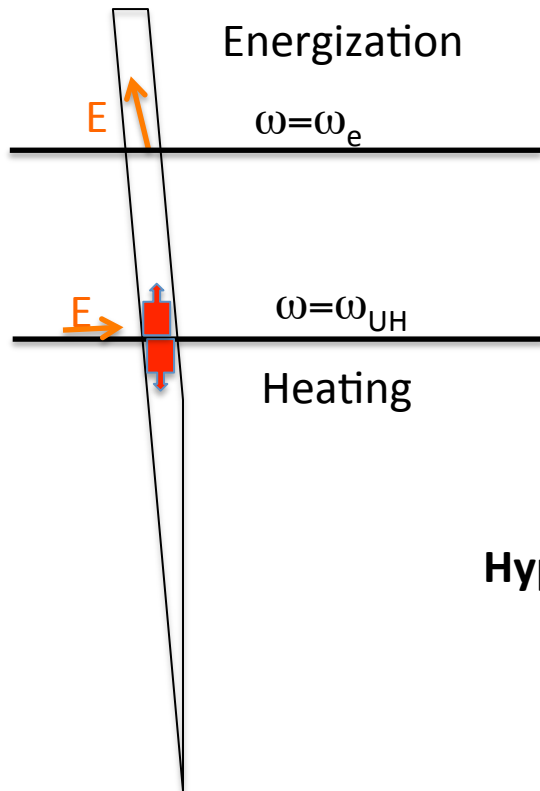


Weak Turbulence



# UH HEATING AND THE ROLE OF DOUBLE RESONANCE $\omega_{UH} \approx n\Omega_e$

Is it related to ECR acceleration and how do we account in the context of our DAIL model?



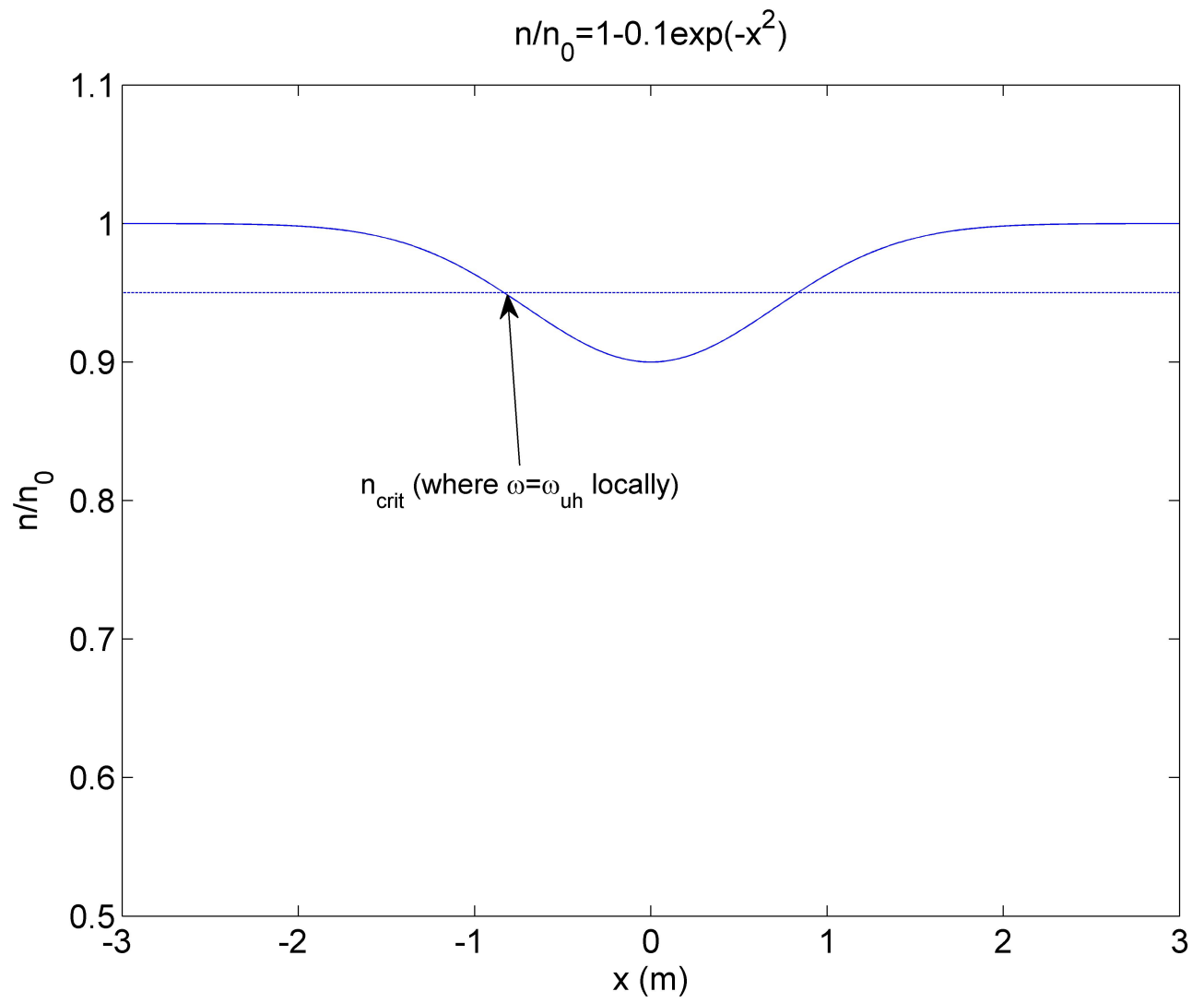
The extent of acceleration depends of heating

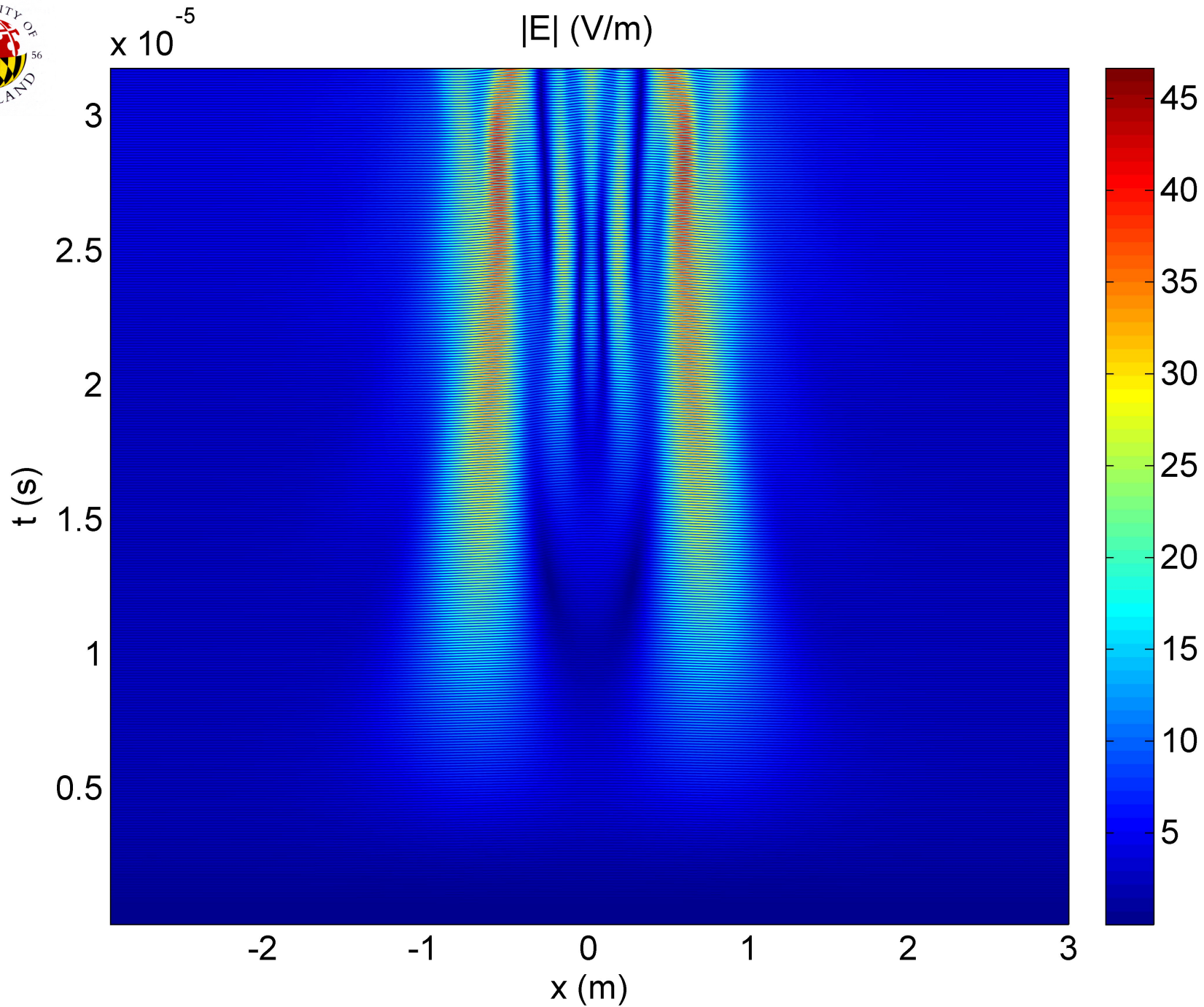
**Hypothesis:** UH heating different under double resonance

**Next :** Two ongoing studies of UH heating



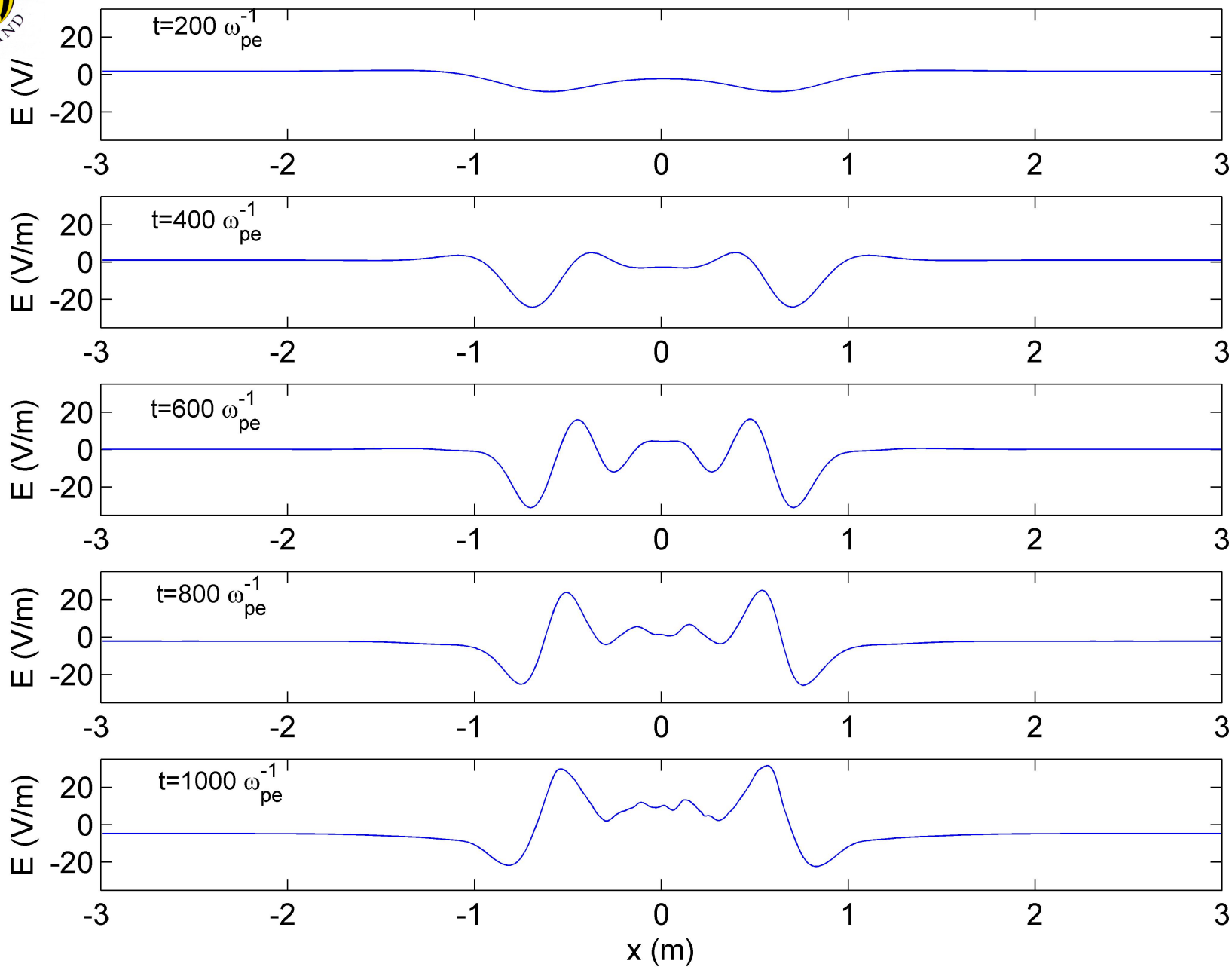
# UPPER HYBRID – RESONANCE ABSORPTION







$$\omega_{pe} = 31.4 \times 10^6 \text{ s}^{-1}, \quad \omega_{ce} = 0.248 \omega_{pe}, \quad \omega_{UH} = 1.030 \omega_{pe}, \quad \omega = 1.004 \omega_{pe}$$





# STUDY ELECTRON HEATING DUE TO ES WAVE GIVEN BY $E_x = E_0 \sin(kx - \omega t)$

Stochasticity analysis  $10^4$  particles

$$m \frac{dv^j}{dt} = -eE_0 \sin(k_x x^j - \omega t) \hat{x} - e \mathbf{v}^j \times B_0 \hat{z}$$

$$\frac{dx^j}{dt} = v_x^j$$

$$\frac{du_x^j}{dt} = -A \sin(u_y^j - \Omega t) - u_y^j$$

$$\frac{du_y^j}{dt} = u_x^j$$

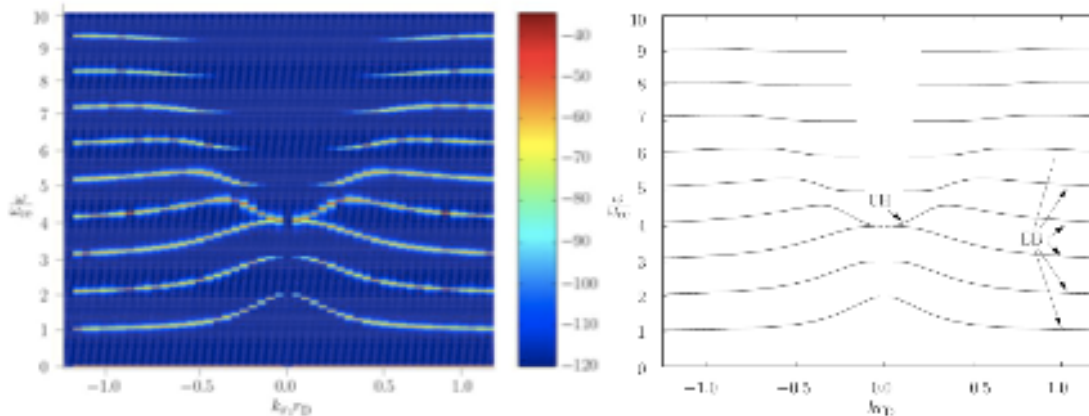
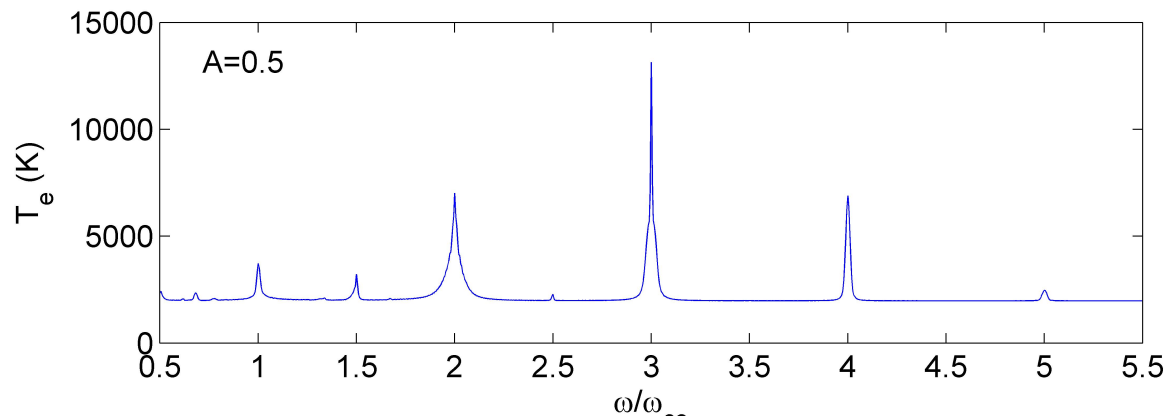


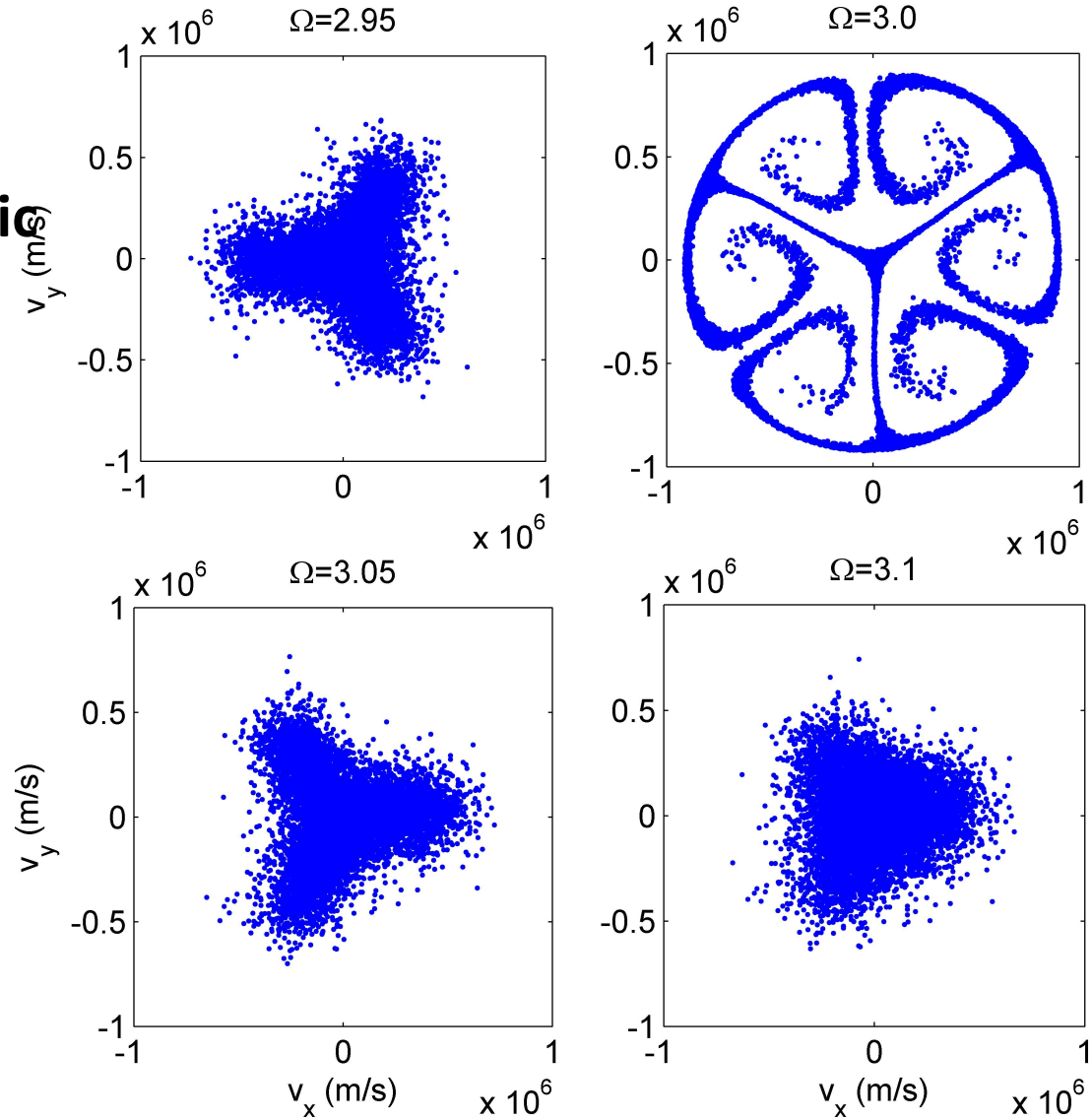
Figure 2: Power spectrum obtained from a Vlasov simulation (left) and theoretical dispersion diagram (right) showing the upper hybrid (UH) branch and several electron-Bernstein (EB) modes at the electron cyclotron harmonics for  $\omega_{UH} = 4\omega_{ce}$ . The wave energy is concentrated to the eigenmodes of the system. After Eliasson (2010).

$A = ek_x E_0 / m \Omega_e^2$ ,  $\Omega = \omega / \Omega_e$ ,  
Velocity norm to  $\omega/k$ ,  $t \rightarrow 1/\Omega_e$



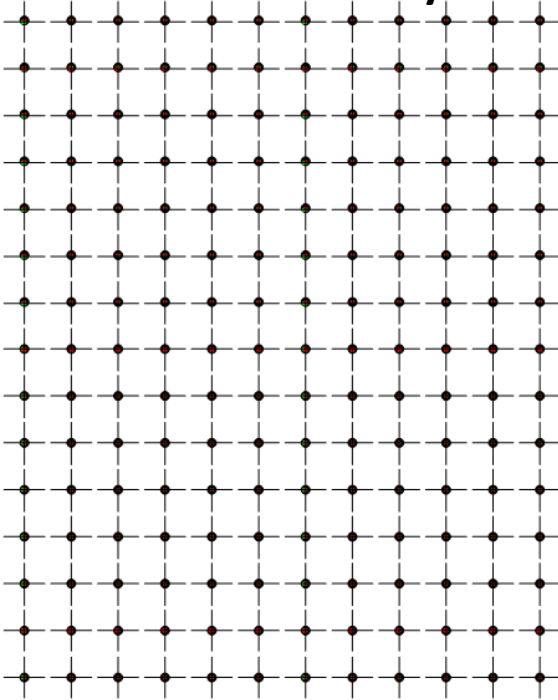
3.5 V/m

# Strongly anisotropic Heating

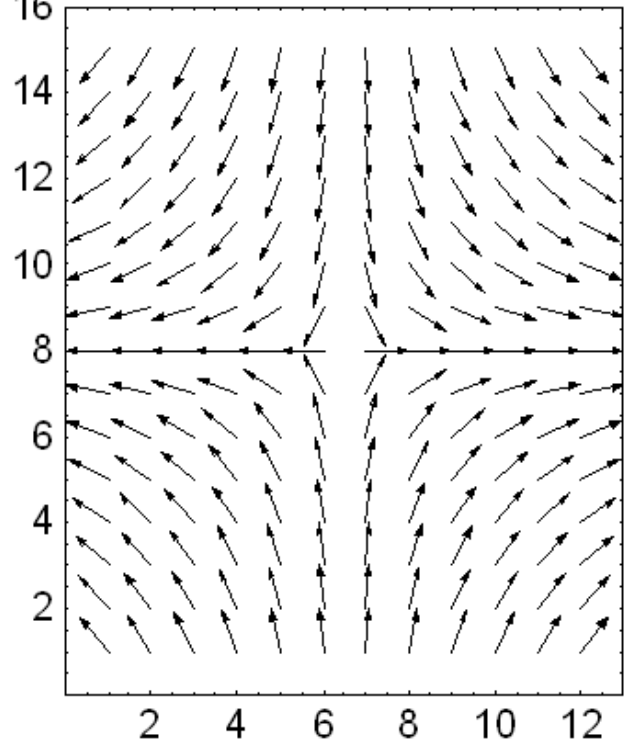


# L=1 OAM Generation with HAARP

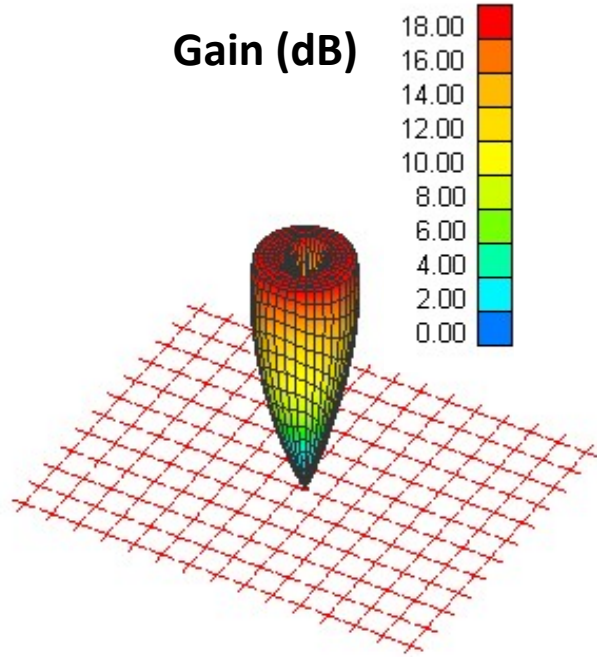
Antenna Array



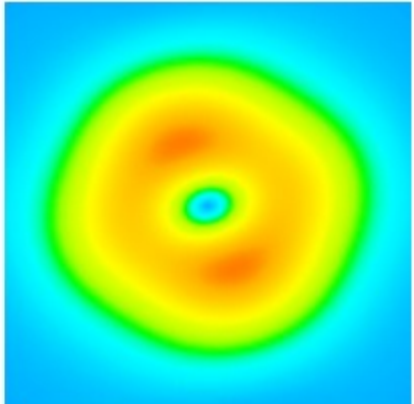
Electric Field Phase



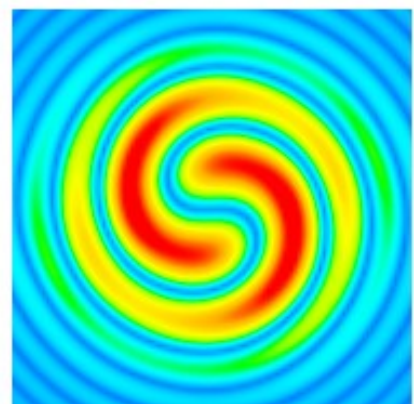
Gain (dB)



Average  
 $|E|$  (V/m)



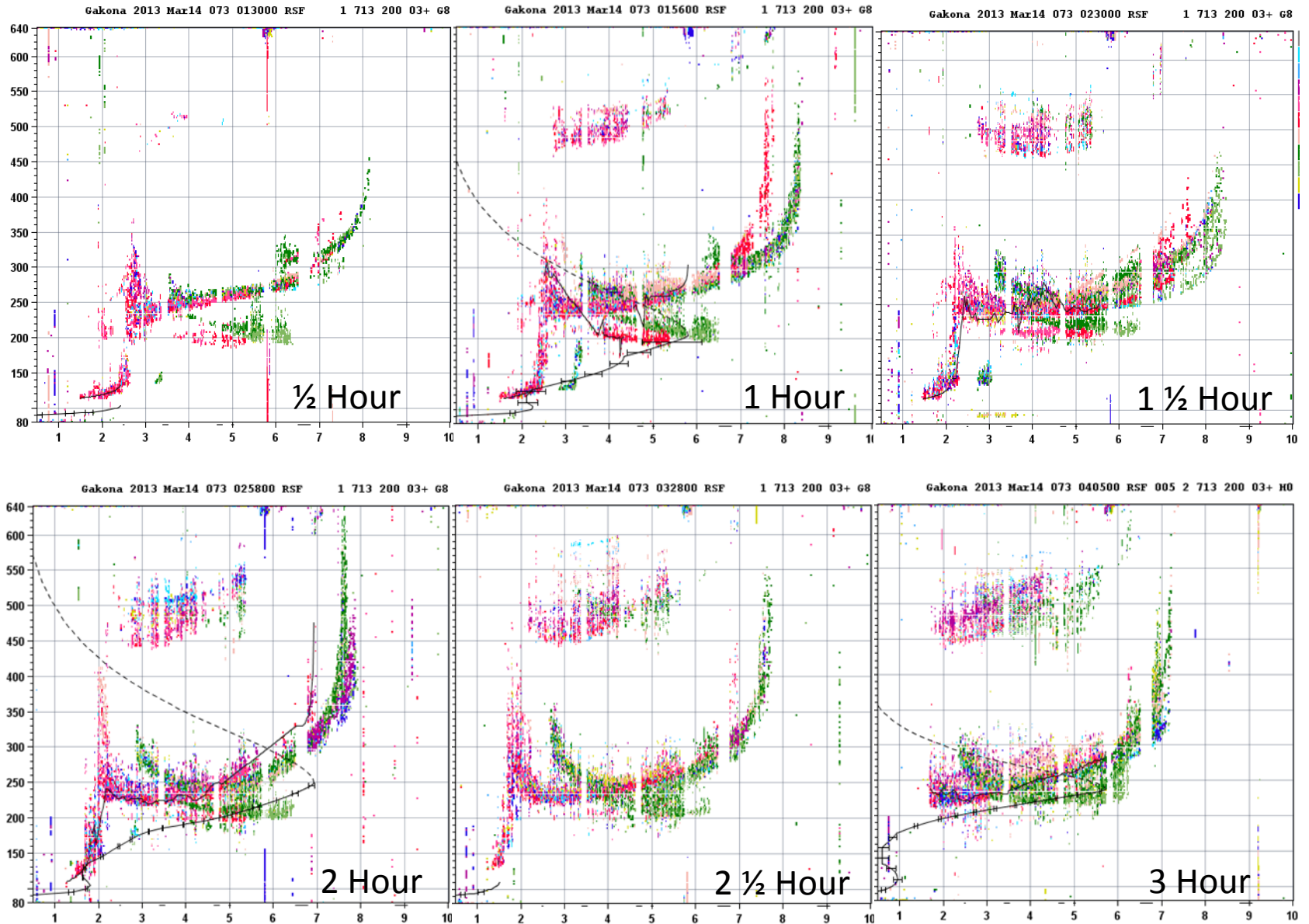
Instant  
 $|E|$  (V/m)



BERNHARDT

14 March 2013 01:30 to 04:00 GMT

# Extended Artificial Ionization with 5.8 MHz Twisted Beam



# **SUPPELEMENTARY SLIDES**

# SEE Spectra

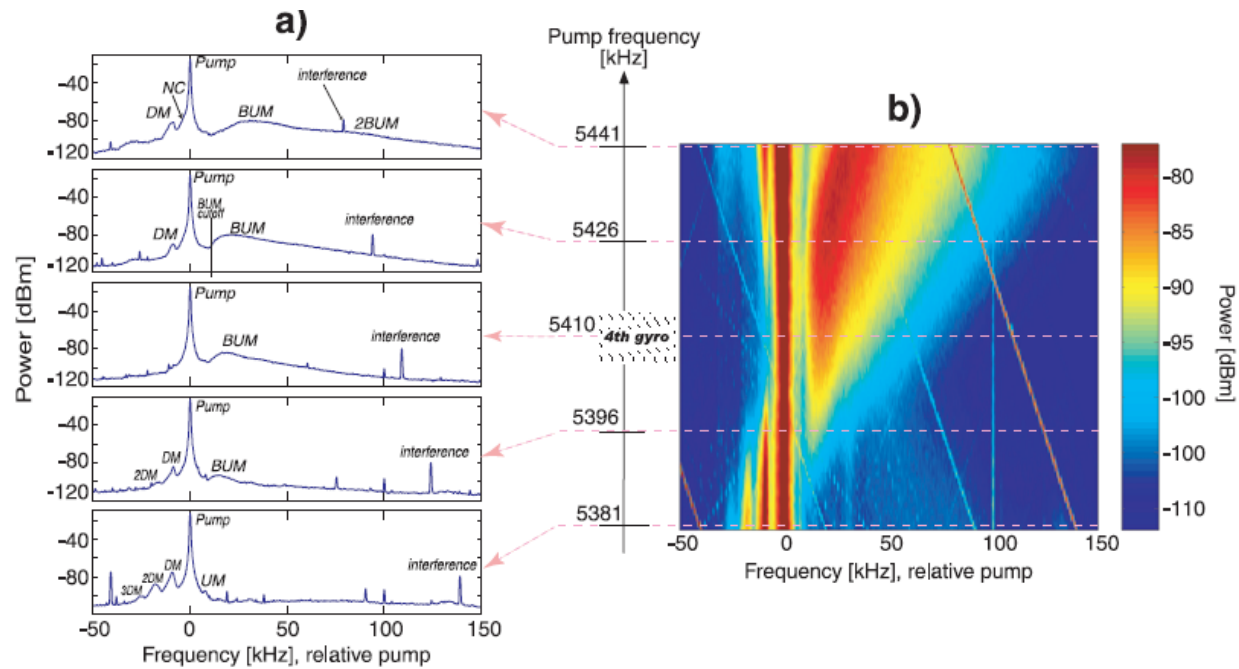
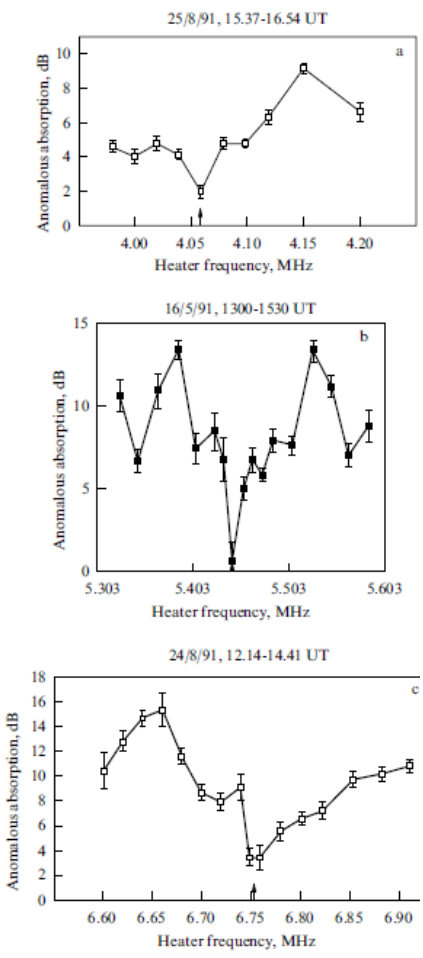


**Figure 3.** (a) The stack of five plots showing SEE spectra for the five different pump frequencies marked on the vertical axis in the middle of the figure. The standard SEE spectral features and the pump are labeled. These spectra are cross sections of the pump relative spectra versus pump frequency two-dimensional plot in Figure 3b. (b) The position of the cross sections are marked with dashed, magenta lines. The estimated range of the local fourth gyroharmonic is shown as a hatched region on the pump frequency axis.

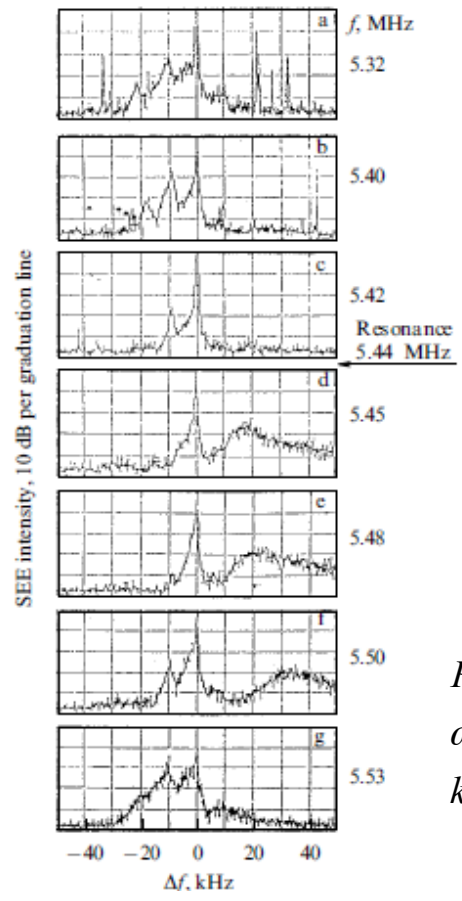
# SuPer-Short Striations

Effects associated with  $\omega \approx \omega_{uh}(z) \approx n\Omega_e$

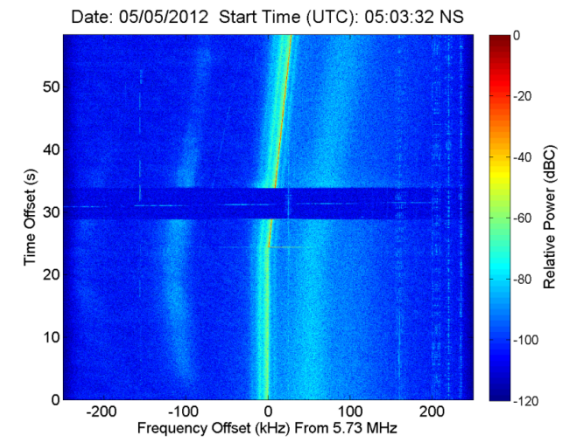
Gurevich Physics-Uspekhi, 2007



Suppression of anomalous absorption



BUM  
Generation of short scale FAI Super-Short-Striations (SSS)



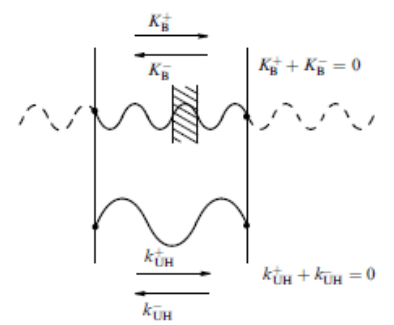
Paul's BUM

Need for four wave interaction – Pump, UH, EB, IA.

$Pump(\omega, k_o = 0), UH(\omega_1, k_1), EB(\omega_2, k_2), IA(\omega_s, k)$

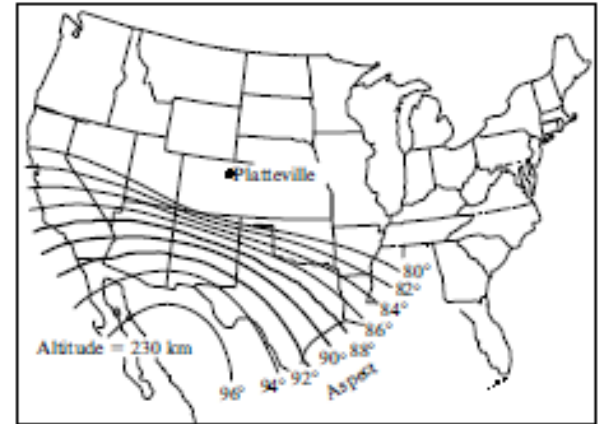
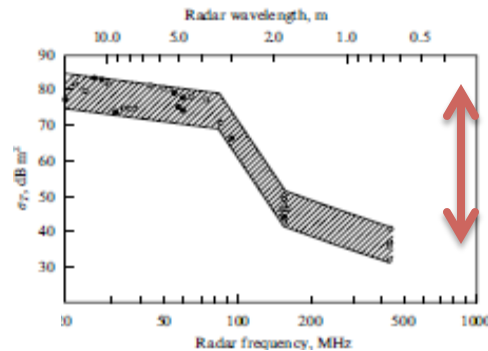
$\omega_1 + \omega_s = \omega = \omega_2 - \omega_s, \rightarrow \omega_2 > \omega$

$k_1 + k = 0 = k_2 - k, \rightarrow k = k_2 \approx O(1/r_e)$



# Raising MUF to GHz

Platteville FAS:



FAS Concept- Aspect scattering. RF transmitted from Tx along the 90° line are orthogonal to FAI and will be observed everywhere at the 90° line. Tx located in the 92° line observed at 88° and vice versa

Middle or equatorial latitude

**Potential answer from physics of ion cloud formation**

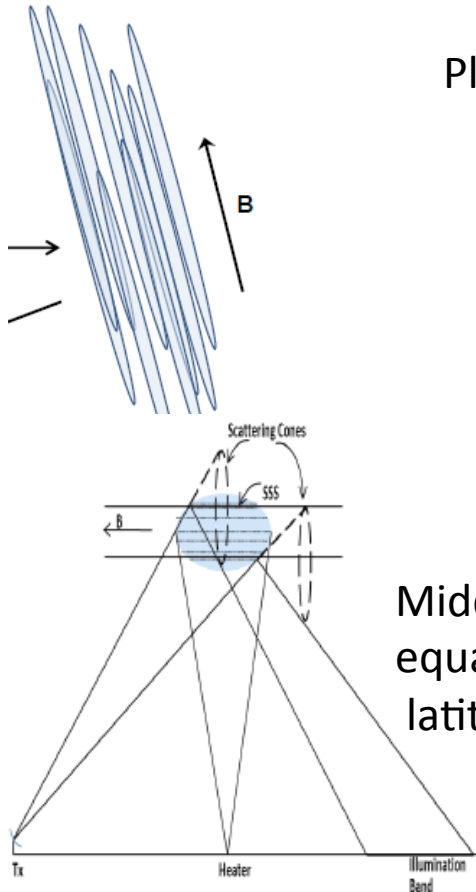
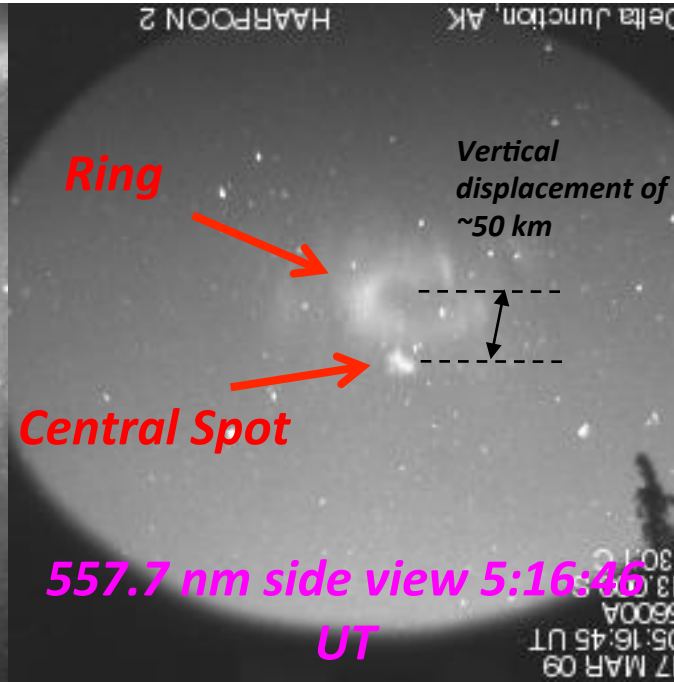
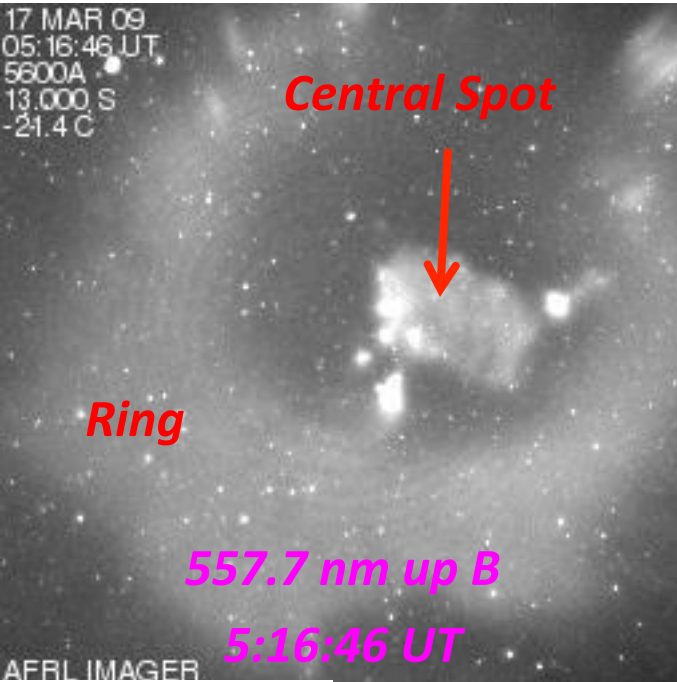


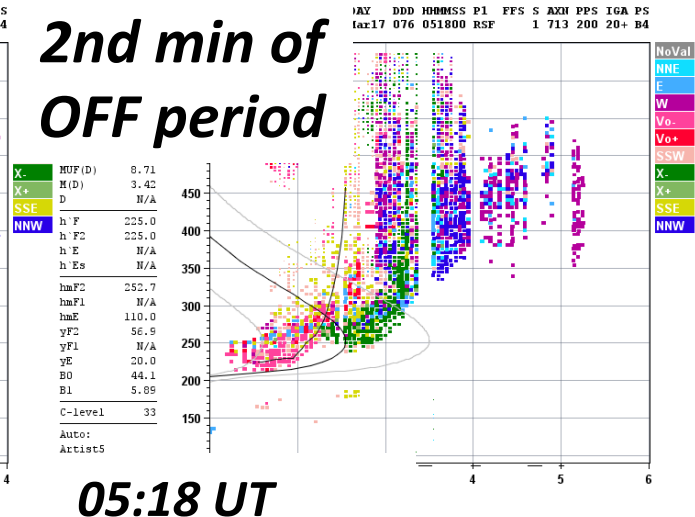
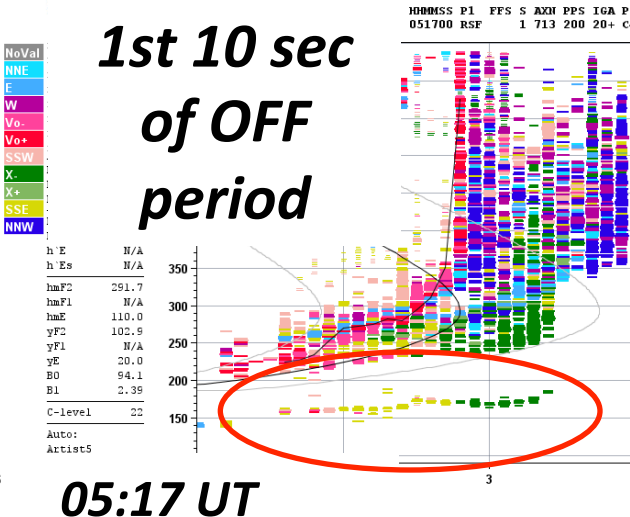
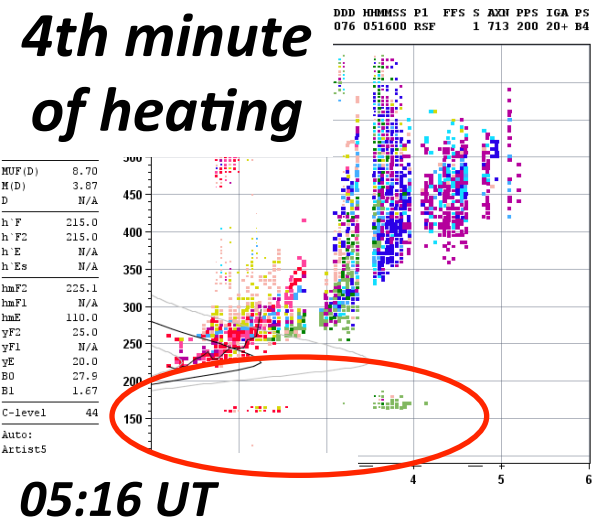
Fig. 1: Schematic of SSS FAS system at GHz.



# Mystery Solved by Multi-Site Optical Observations: March 2009



- Combined data sets indicate presence of artificial plasma sufficient to interact with heater beam
- At altitudes with no significant natural plasma!



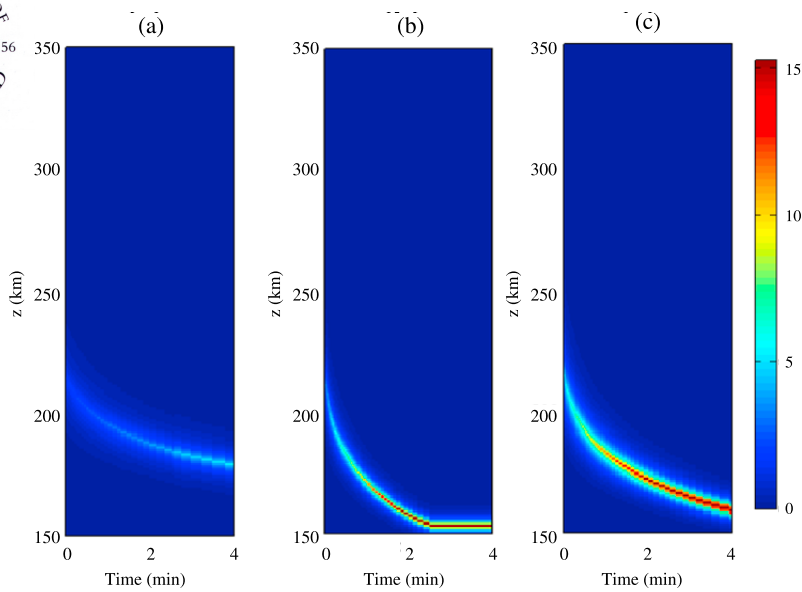
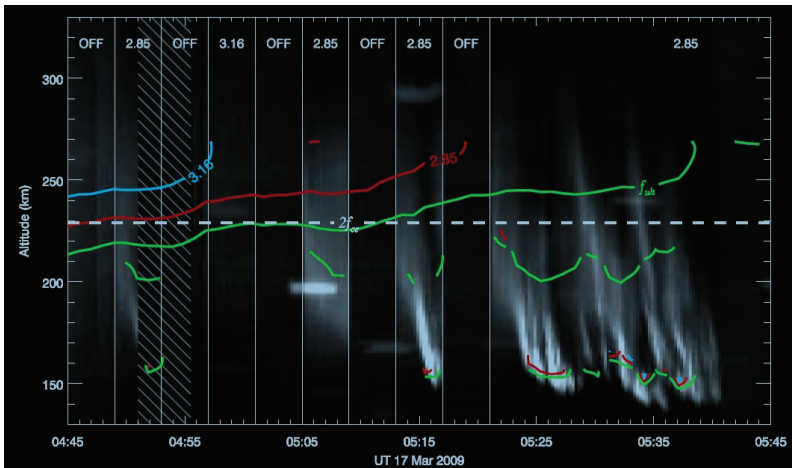
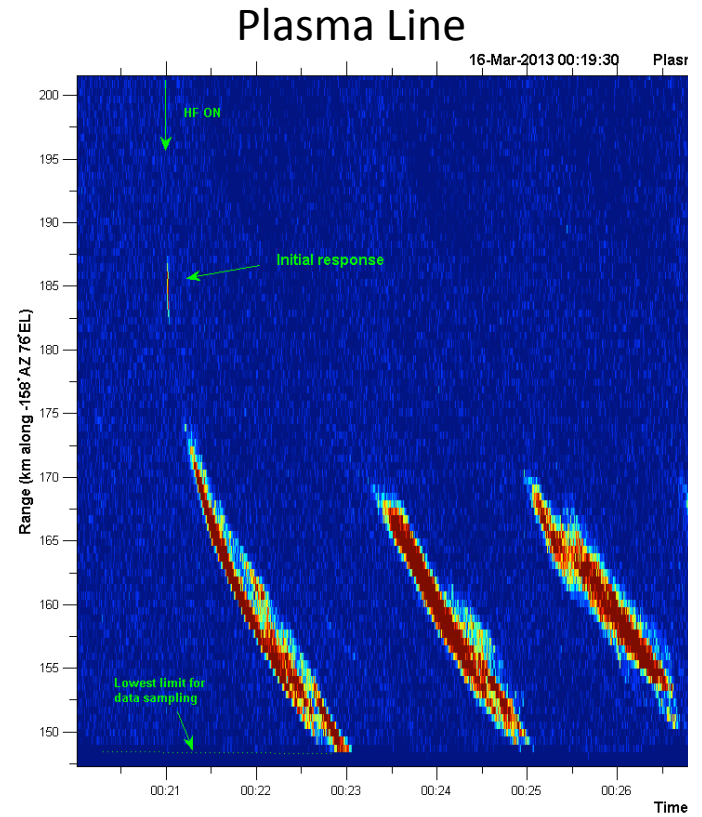
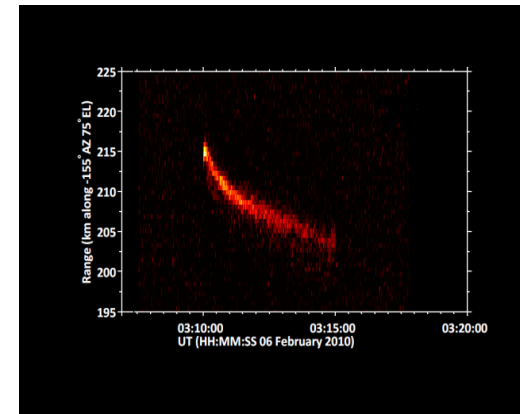


**Figure 13.** Green line emission as derived from simulation for different input wave amplitude and initial electron thermal energy: (a)  $E_0 = 1$  V/m,  $T_e = 0.4$  eV, (b)  $E_0 = 1.5$  V/m,  $T_e = 0.4$  eV, and (c)  $E_0 = 1$  V/m,  $T_e = 0.6$  eV.



Descending ion-line and plasma line structures observed with UHF radar during heating.

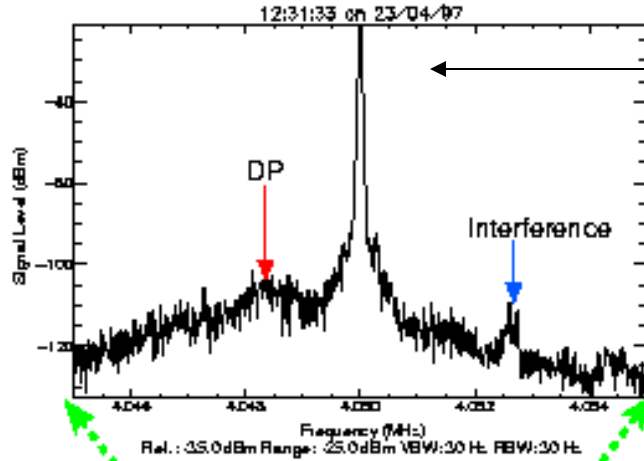
Watkins



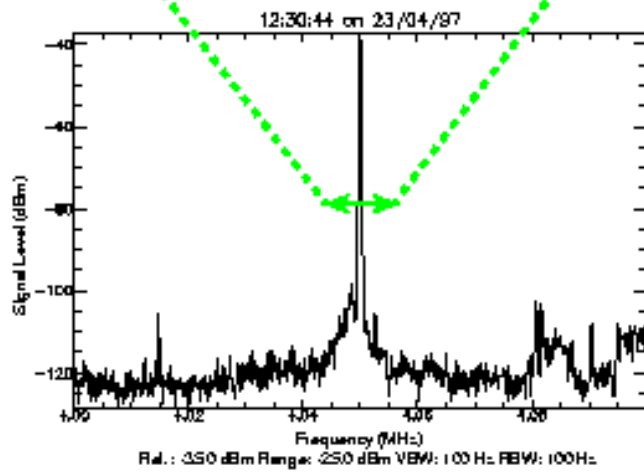
T. Pedersen et al. 2010

Ion Line

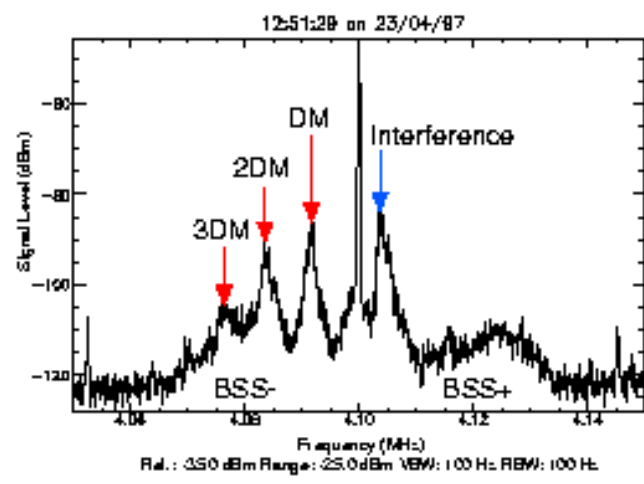
# Stimulated Electromagnetic Emissions (SEE)



HF transmit frequency



**3rd Electron Gyroharmonic**



**Above Gyroharmonic**

Gyroharmonic  $\approx 1.38$  MHz in F-layer

are weak radio waves produced in the ionosphere by HF pumping.

(Honary et al., Ann. Geophysicae, 1999)

# SEE Spectra

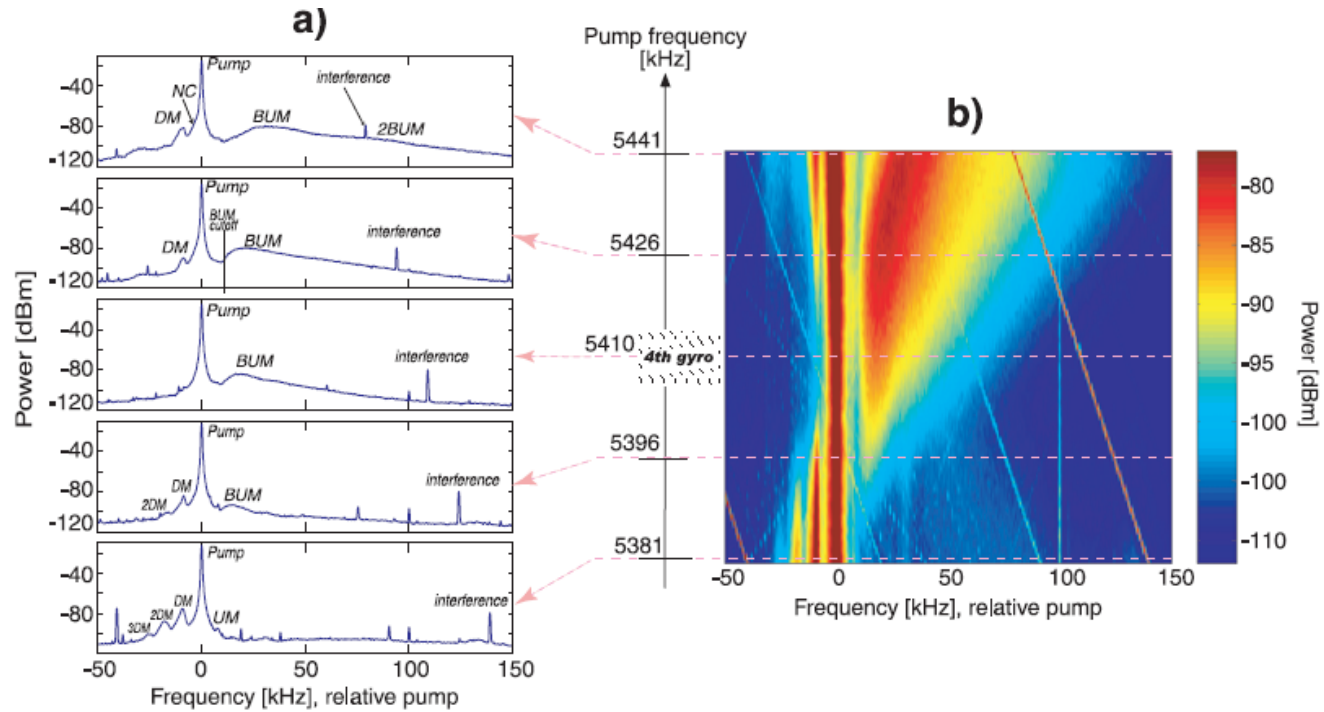
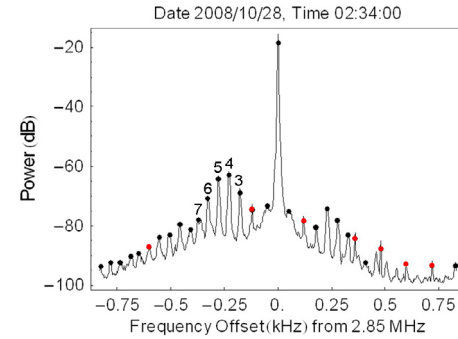
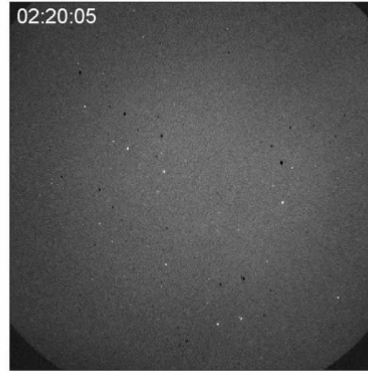
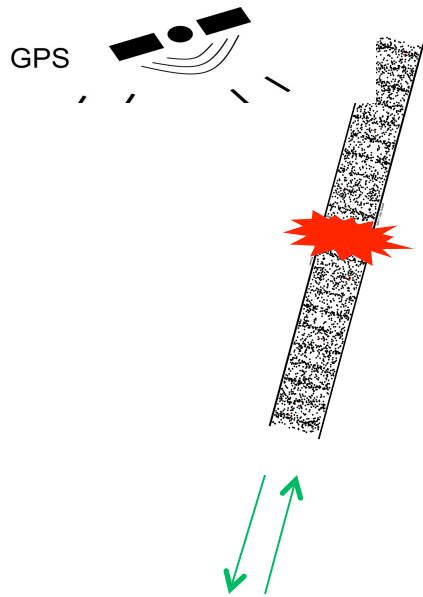


Figure 3. (a) The stack of five plots showing SEE spectra for the five different pump frequencies marked on the vertical axis in the middle of the figure. The standard SEE spectral features and the pump are labeled. These spectra are cross sections of the pump relative spectra versus pump frequency two-dimensional plot in Figure 3b. (b) The position of the cross sections are marked with dashed, magenta lines. The estimated range of the local fourth gyroharmonic is shown as a hatched region on the pump frequency axis.

# DIAGNOSTIC INSTRUMENTATION

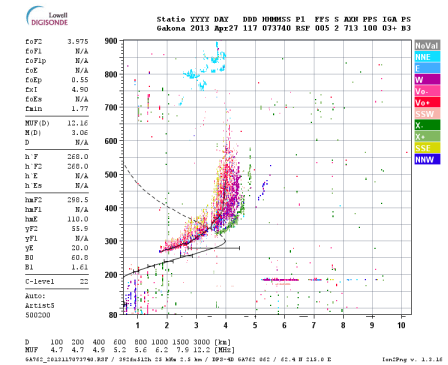
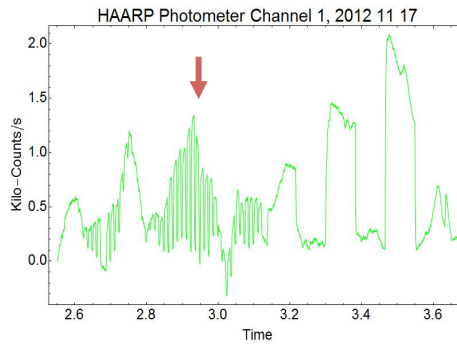
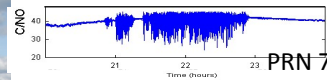
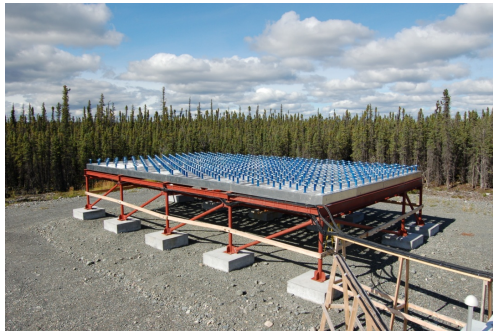


SEE

630 nm Artificial Plasma  
Glow Discharge Ionization

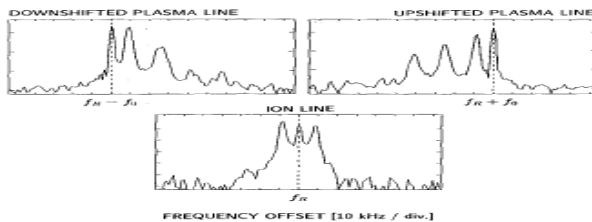
Eight channel HF receivers, NRL

Optics: All-sky imager ,Telescopic imager  
Photometers ,14 ft Optical Dome  
Tomography Chain ,Cordova -> Kaktovik

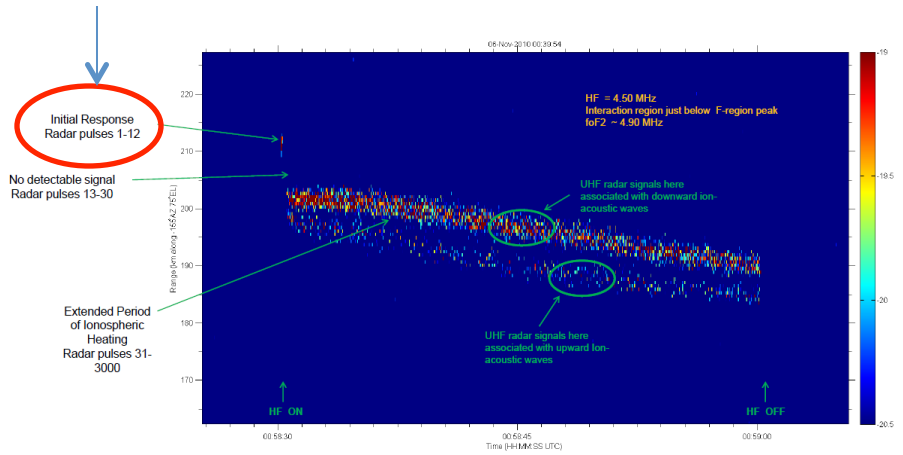
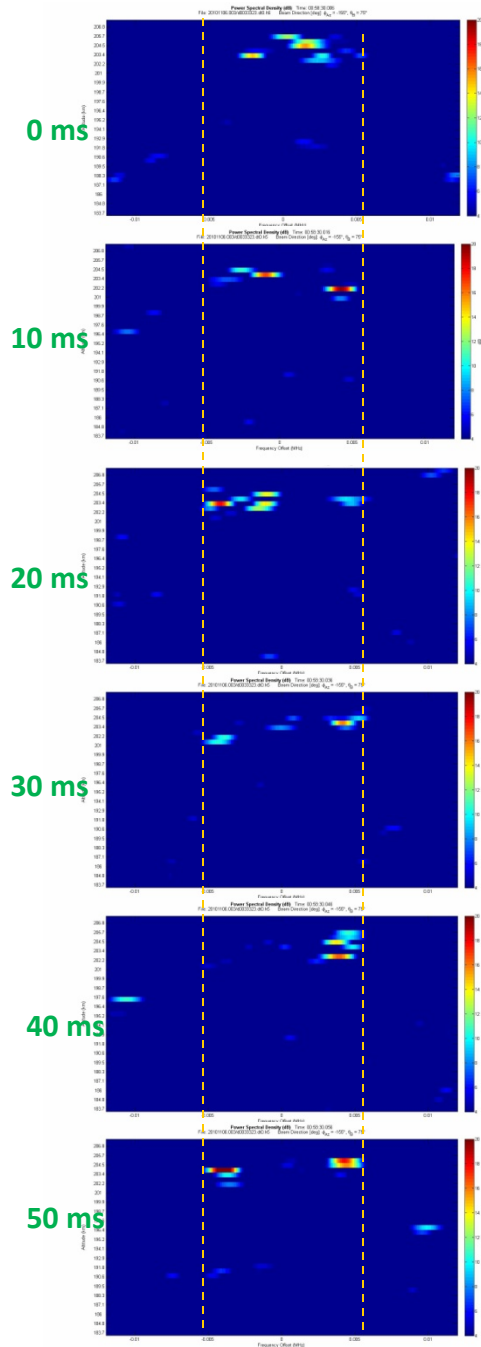


Ionosonde

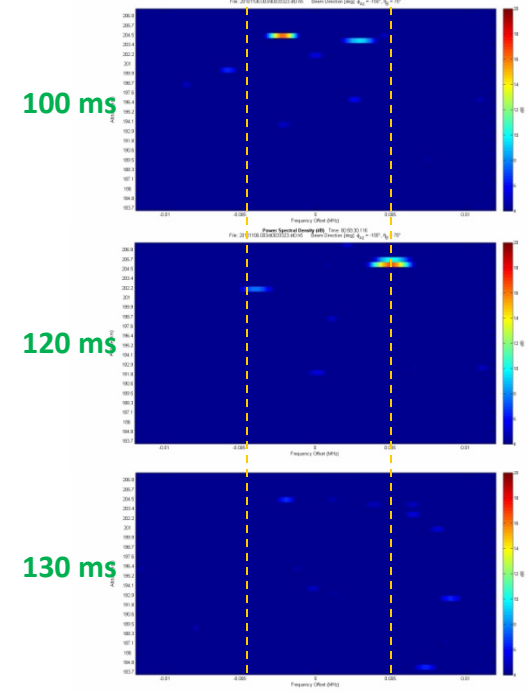
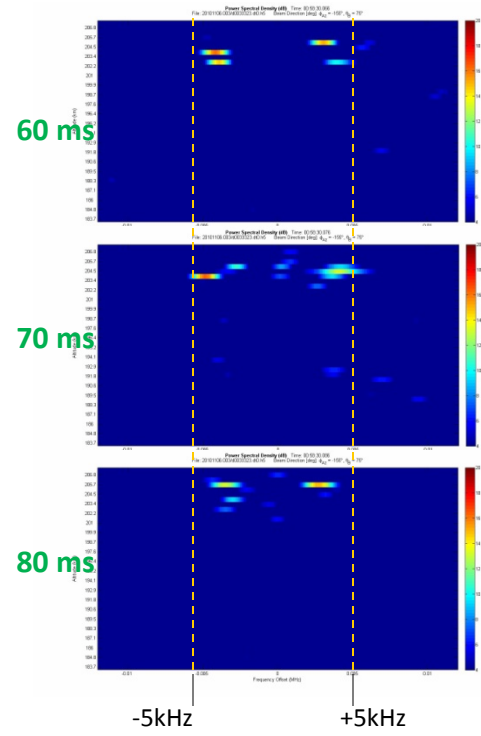
UHF Radar (446 MHz)

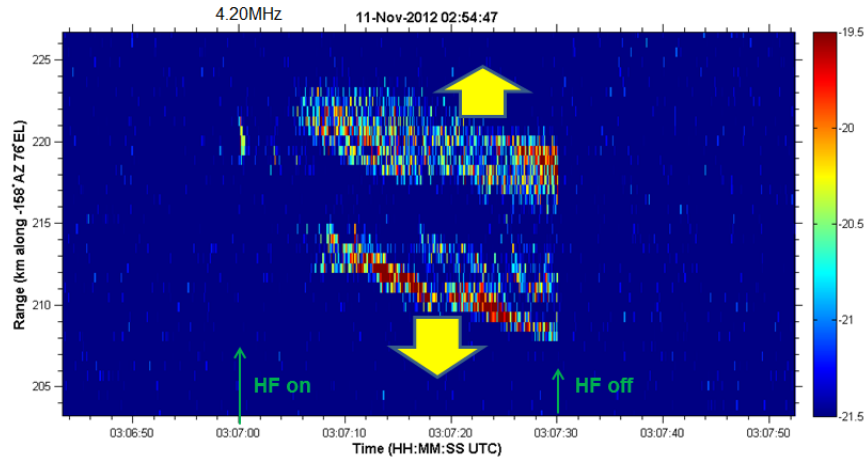


# UHF Power Spectra During Initial Response Time (First 12 pulses after HF turn on - 120 milli-sec)



← 30 sec HF on time →

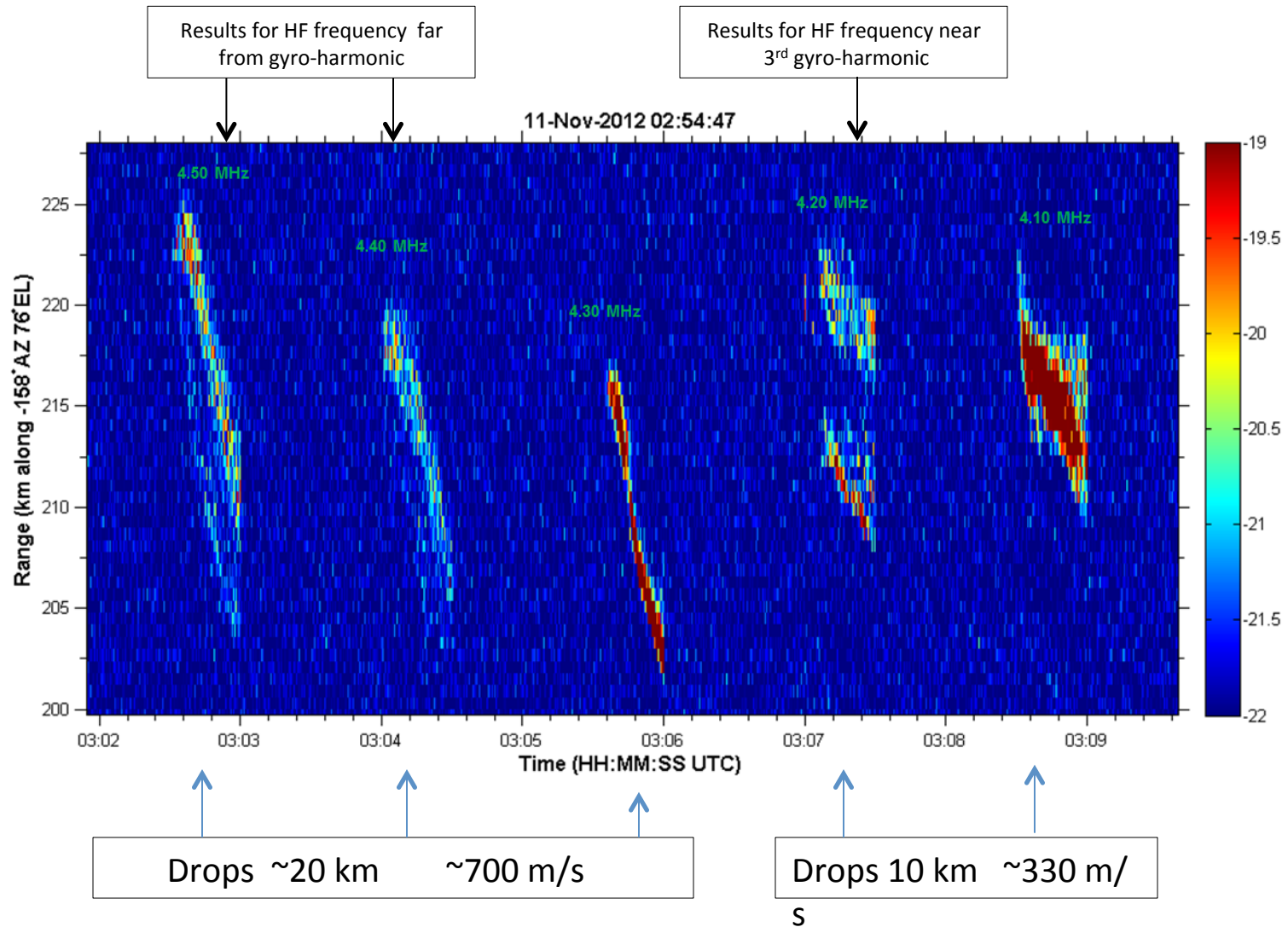




## Experimental results that suggest:

Large-scale density changes maximized for HF frequencies far from gyro-harmonics

Results for 4 HF frequencies near the 3<sup>rd</sup> Gyro Harmonic      HF power cycled: 30secs on 60 secs off

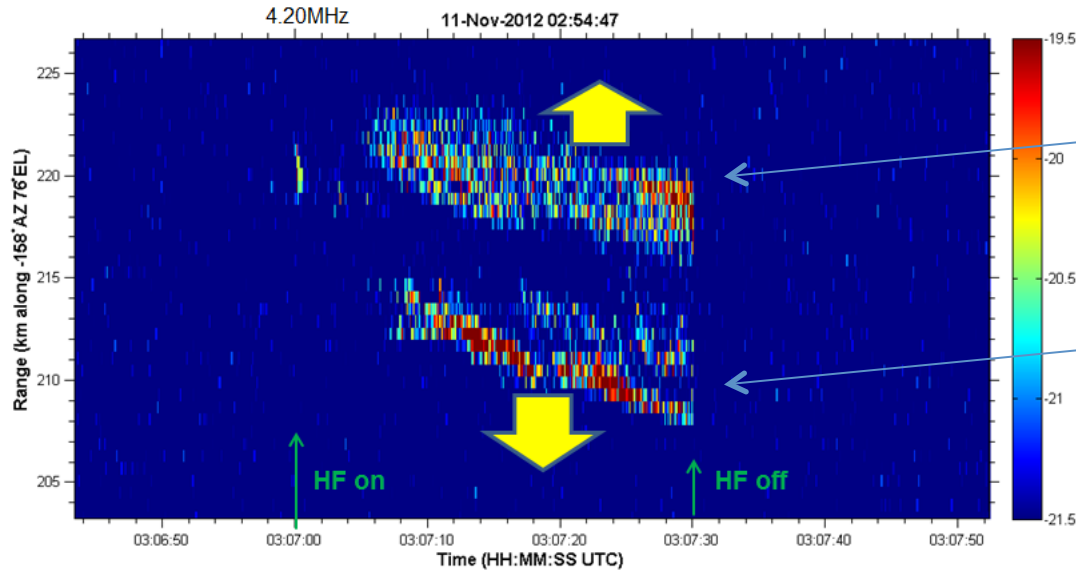




Topic 4: UHF Radar Doppler Power Spectra Observations

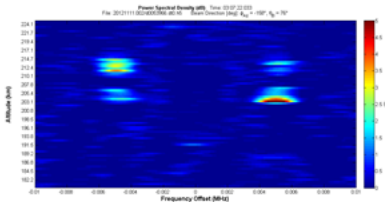
Enhanced Ion-Line Doppler Spectra for 4.20MHz  
(close to 3<sup>rd</sup> Gyro-Harmonic)

*New Results:* Two scattering structures with preferentially-directed ion-acoustic wave directions



Upward ion-acoustic waves

Downward ion-acoustic waves



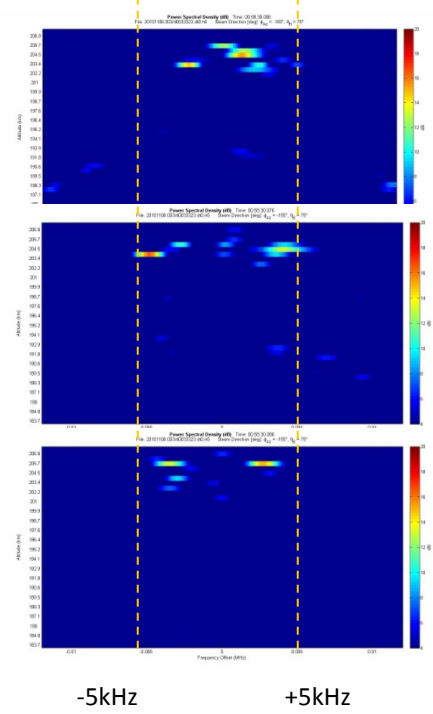
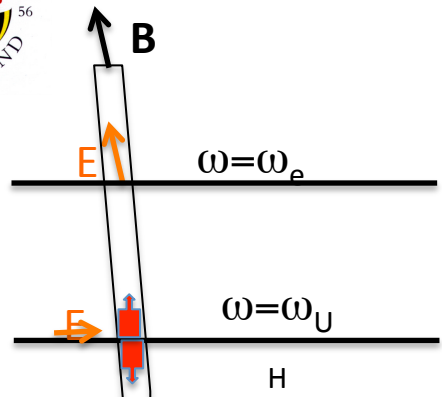
Power-height-time plot of HF-enhanced ion-line signals. Close to 3<sup>rd</sup> gyro-harmonic signals split into two layers. Doppler spectra (example to left) show strong asymmetries that indicate mainly upward propagating only ion-acoustic waves in the upper layer. The downward layer is associated with primarily downward propagating ion-acoustic waves..

**HF Power Cycle**

30 secs on

60 secs off

The above spectral asymmetries are interpreted to be the result of electron flow upward and downward from the HF interaction region as indicated by the yellow-colored arrows.



**Multi-time and length scale code (DAIL code suite- Eliasson et al. JGR 2012):** (i) El. Accel in SLT, (ii) Transport model for accel. El., (iii) ionization (iv) Chemistry package (recomb., excit...)  
**Input:** (i) HF E at 100 km (ii) Ambient density (iii)  $T_e$   
**Output:** (i) Temporal evolution of density and optical emissions (ii) Supra-thermal EDF

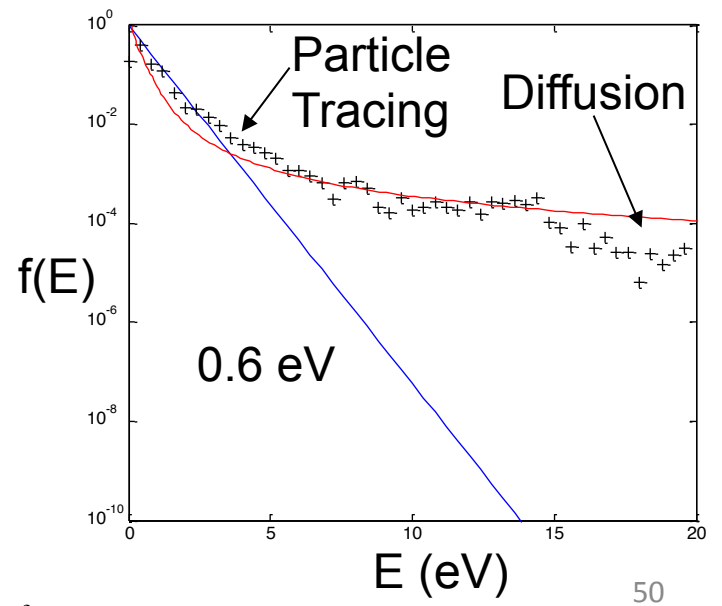
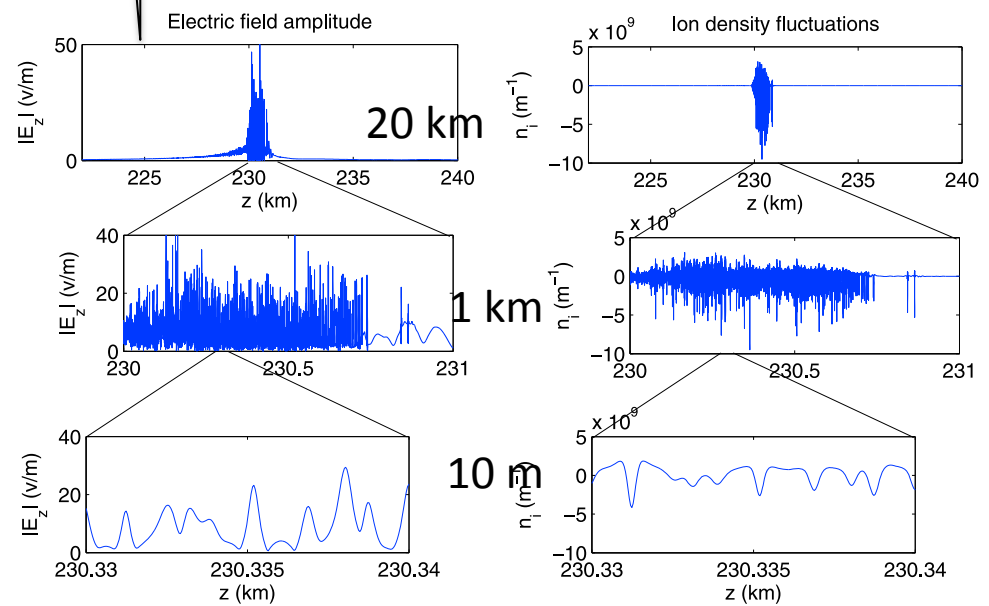
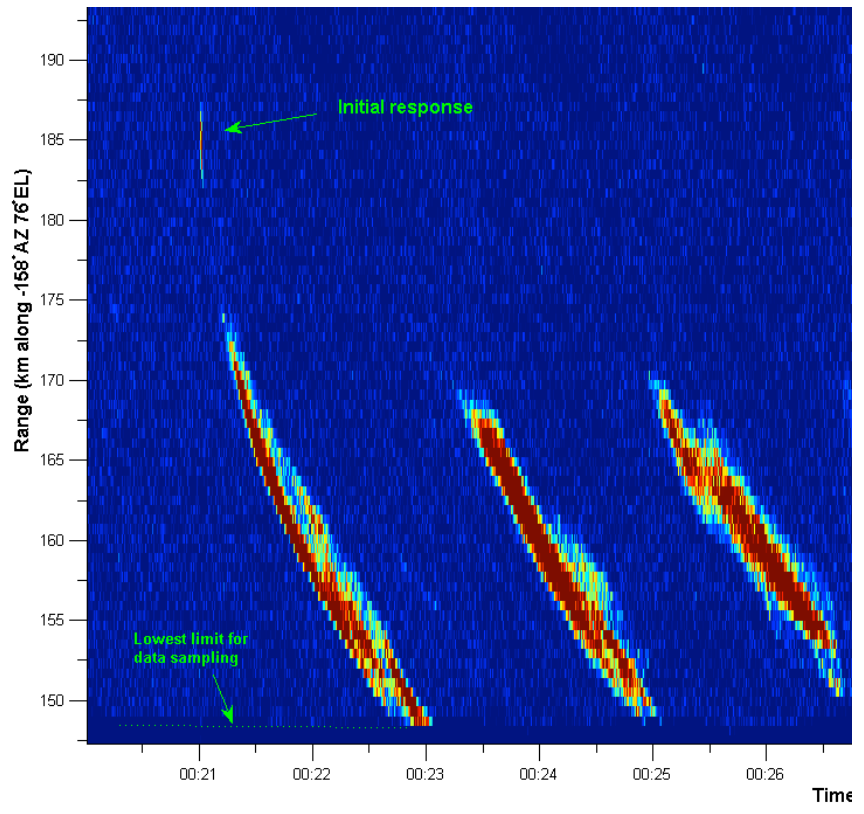
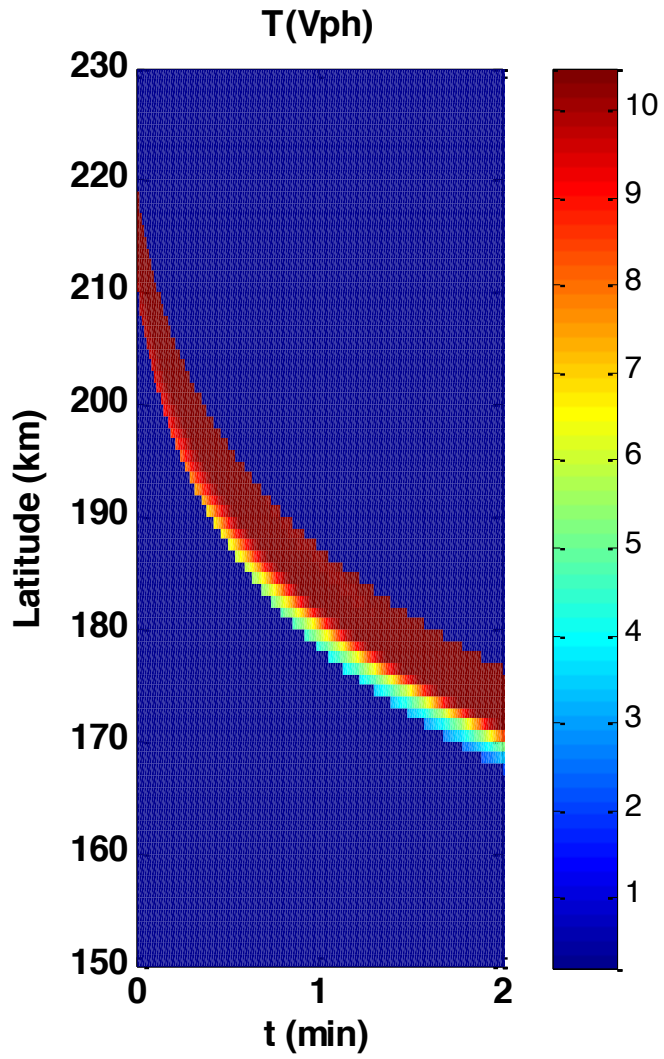
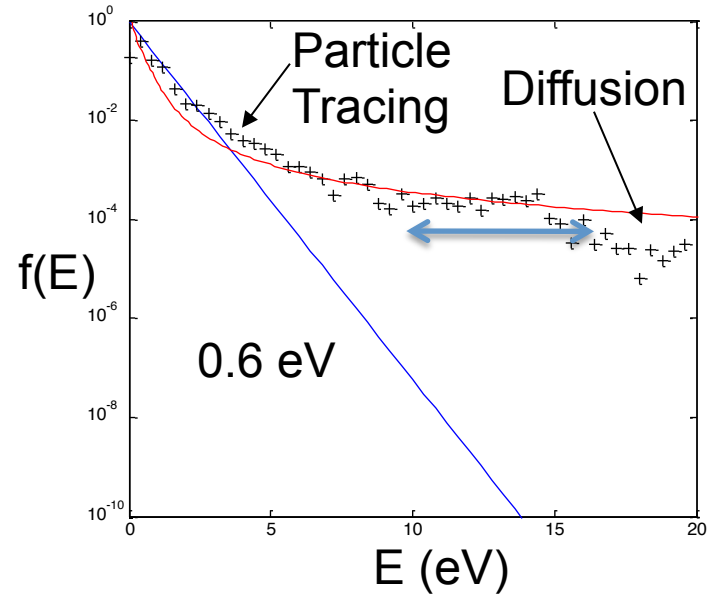
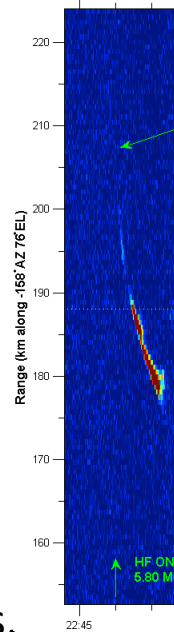
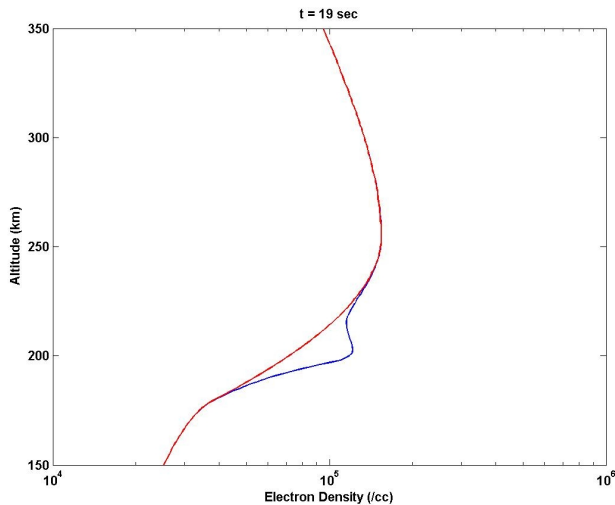


**Figure 2.** The amplitude of  $E_z$  and slowly varying ion density fluctuations  $n_i$  at various altitudes, for  $E_0 = 1.5\text{V/m}$ .



# PLASMA LINE ENHANCEMENT



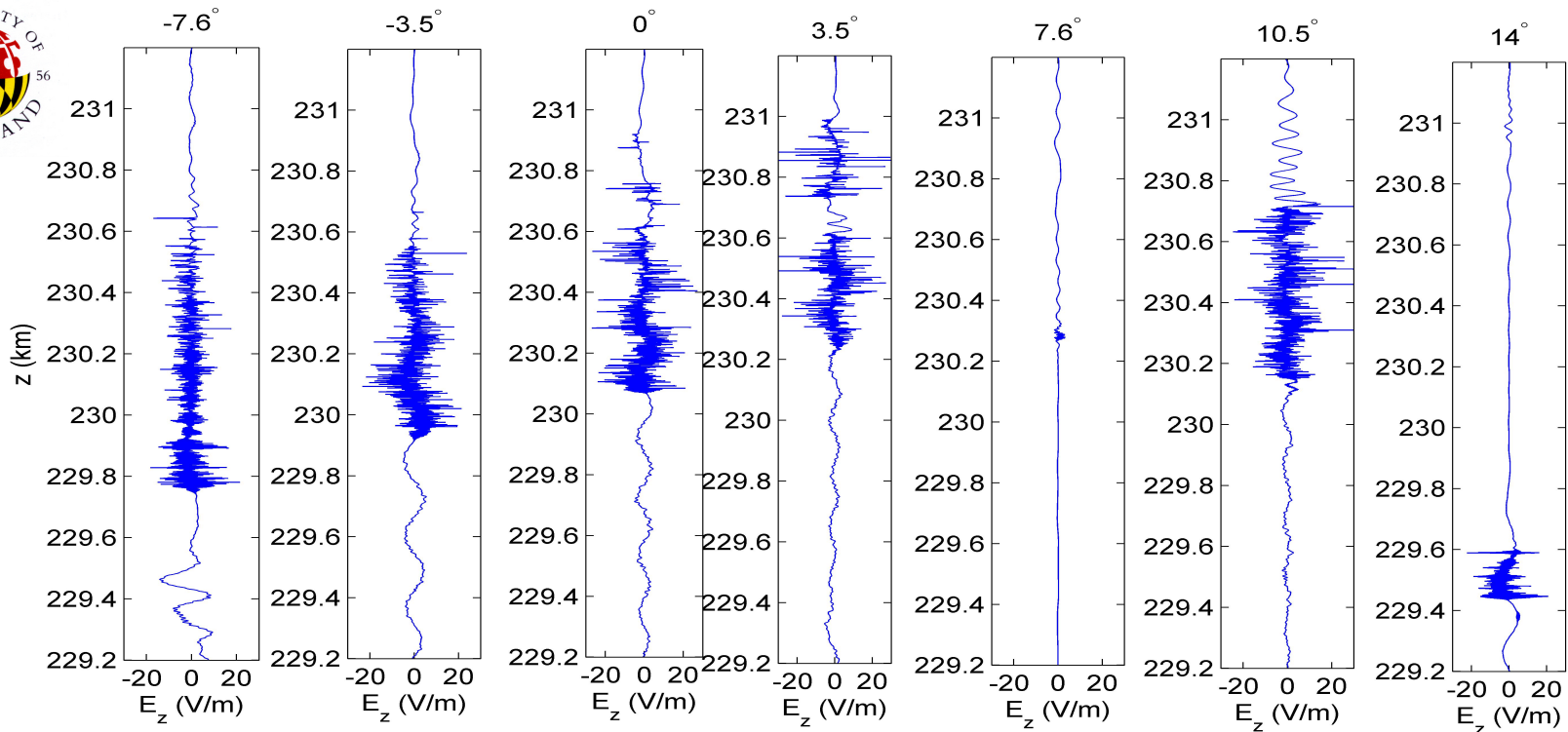
Enhancement due supra-thermal tails. Similar to Arecibo enhancement by photoelectrons but much stronger. The ionizing wave includes large  $T_e/T_i$  plasma and hot electron tails. Enhancement stops at low altitude when collisional damping dominates over Landau.

**Classic signature of non-equilibrium plasma with supra-thermal tails**

$$\frac{\langle E^2 \rangle}{8\pi} \approx \frac{8ne^2}{\omega_e} \int_{k_1}^{k_2} dk k \frac{F_T(\omega_e/k)}{|F_e'(\omega_e/k)|}$$

$$R < \frac{V_T^2/V_e^2}{/n(V_E/\alpha V_e)} \rightarrow (\lambda_R/\lambda_D)^2$$

$$\text{if } \nu < \omega_e u_{ph}^2 F'(u_{ph})$$



O-mode, 1V/m amplitude, electron temperature 0.4 eV, and different angles of incidence, B field *at*  $14^\circ$  to the vertical line (same parameters as JGR 2012).

$E_z$  amplitude  $t=1$  ms for different angles of incidence. The case  $7.6^\circ$  corresponds roughly to the Spitzze angle  $8.1^\circ$ . Also at  $7.6^\circ$  there is an accumulation of electrostatic waves due to absorption (called southward process by Mjølhus 1990). The O mode turning point is at  $z=231.0$  km and the upper hybrid resonance layer at  $z=223.8$  km (outside the range of the plots).

